REVIEW ARTICLE

Anti-cancer Drug Delivery Using Metal Organic Frameworks (MOFs)

Mihad Ibrahim, Rana Sabouni and Ghaleb A. Husseini*

Department of Chemical Engineering, Faculty of Engineering, American University of Sharjah, Sharjah, United Arab Emirates

Abstract: Cancer is the uncontrolled growth of cells in the body and is considered as one of the major causes of death globally. There are several cytotoxic chemotherapeutic agents used to treat cancer including methotrexate, 5-fluorouracil, cisplatin, tamoxifen, doxorubicin and others. Although billions of dollars have been spent on cancer research to develop these chemotherapies, it still remains a major illness for mankind partly due to the shortcomings of these therapies. These shortcomings include low targeting specificity, severe side effects (due to high doses) and poor pharmacokinetics. To avoid these drawbacks, anti-cancer drug delivery systems have been developed recently using nanocarriers including liposomes, micelles, polyelectrolyte capsules and others.

One of the recent class of nanoparticles investigated for chemotherapeutic use are metal organic frameworks (MOFs) which are hybrid polymers that consist of metal ions or clusters and organic ligands. MOFs are used in many applications including gas/vapor separation, gas storage, catalysis, luminescent materials, and biomedical imaging. These structures have additional features that promote their use as drug carriers in the biomedical field. First, they are nontoxic, biodegradable and have the ability to carry high loadings of the anti-neoplastic agent due to their porous nature. Also, they have well-defined crystalline structures that can be characterized by different analytical techniques and their sizes are suitable to control their *in vivo* drug release.

This paper reviews the methods used to synthesize MOFs and their recent use as antineoplastic drug delivery carriers.

"The published manuscript is available at EurekaSelect via http://www.eurekaselect.com/openurl/content.php?genre=article&doi=[10.2174/0929867323666160926151216]."

1. INTRODUCTION

Cancer is a deadly disease characterized by the rapid growth of abnormal cells in the body [1]. Its increased spread is attributed in part due to the rapid growth of the population along with the bad lifestyle habits including smoking, eating fast foods and the lack of physical exercises [2]. In 2007, cancer killed about 7.9 million people all over the world and this number is increasing annually [3]. About 14.1 million new cancer patients were diagnosed in 2012 and 8.2 million death cases were reported by the International Agency for Research on Cancer [4].

Further epidemiological studies were carried out and showed that the number of cancer mortalities is expected to reach 13.1 million by 2030 [5]. The most common cancer among males is lung cancer, while breast cancer is the predominant cancer among females [4].

There are essential differences between healthy and cancerous cells. Cancer cells grow fast and they lack a mechanism of cell death, forming a tumor [6]. More dangerously, some of the diseased cells can break away from the tumor and move through the blood stream to other parts of the body. In this case, they may migrate among healthy cells and start proliferating in a new location. Contrary to malignant cells, when normal cells divide, an equal number dies in the process because they possess a mechanism to induce the programed death of old cells [7].

Despite differences in proliferation and multiplication, cancer and healthy cells are similar in many respects. Biochemical properties at the subcellular level related to the cell's surface are used to distinguish between normal and malignant tissues [7, 8]. The first difference between cancer and normal cells is that normal cells form a monolayer, i.e. a sheet, whereas cancer cells accumulate into multilayers [9]. Also, cancer cells many have fingerlike outcrops on their surfaces [7]. Another distinction is that various cancer cells have the ability to remove protease enzymes which are responsible for the protein digestion process [10]. The effect of these enzymes is to stimulate the cells to grow and in their absence, normal cells stay inactive [11].

The biochemical differences mentioned above could be useful in cancer treatment. They are capable of paving the way to discover therapies that are selective to the cancer cells while having little or no effect on the normal cells.

There are different ways to control and treat cancer depending on its stage, location and the health of the patient [12]. Solid cancer tumors are resected surgically and afterwards, the patient is exposed to radiation therapies to get rid of any cancer cells not removed by surgery. The principle disadvantage of this method is that some of the tumors could not be removed completely and hence are capable of spreading beyond the diseased tissue or organ, causing metastasis in the process [13].

In 1900 and after clearly understanding the progression of tumors, the German chemist, Paul Ehrlich, introduced the new term "chemotherapy". He defined it simply as treating diseases with chemicals [14]. He carried out many experiments on animals to examine the effect of various chemicals against several cancers. In his trials, he referred to chemotherapy as "dye therapy" [15], as he tried to use aniline dyes and alkylating agents in his treatments. Unfortunately all of his attempts failed in regressing tumor growth. Until the 1960s, the prevalent treatment methods for cancer were surgery and radiotherapy [14].

Studies later found that many cancers could not be treated using these treatments (resection/ radiotherapy) and they were ineffective in controlling the metastasis of the disease into other organs. However, it was shown that adding a chemotherapy regimen to the traditional treatments could in some cases solve the metastasis problem even if the cancer was in an advanced stage [14]. The main effect of the chemotherapy is to prevent the proliferation of cells so it affects both cancerous and healthy tissues [16]. This cancer treatment modality proved to be promising, first, in patients suffering from breast cancer as the results revealed that the toxicity of the anti-neoplastic agent towards cancerous cells was higher than those suffered by healthy cells [14].

The development of anti-cancer chemotherapy started in 1930s after the First World War using murine tumors experiments [6]. When murine tumors were exposed to a dose of sulfur mustard gas followed by nitrogen mustard, a fast remarkable reduction in tumor size was observed. After a decade, Goodman, Gilman, Allen and Philips investigated the effect of nitrogen mustard on tumors [17] and suggested the use of low doses of hydrochloride salt solution of nitrogen mustard

injections to restrict and reduce the size of lymphatic tumors [6]. After 20 years of the investigation, the first *in vivo* experiments were carried out by Gilman. The results showed a noticeable effect of the cytotoxic drug (nitrogen mustard) on the lymphoid tissues [17].

These ideas assisted in investigating other drugs for their anti-cancer activity because earlier experiments showed that abnormal cells in tumors are more susceptible to the chemical agent used. Further studies were conducted to test nitrogen mustard as a cytotoxic agent. The mechanism of drug delivery in this case was dictated by the effect of nitrogen mustard which covalently linked alkyl group with deoxyribonucleic acid (DNA) on purine [6]. The site at which cross-links formed matched where cancer cells died [18]. One of these alkylating agents is cyclophosphamide which is used to cure several types of cancer including leukemias, lymphomas and some solid tumors. It was observed that cyclophosphamide had a short term treatment and eventually cancer cells started resisting this chemotherapy treatment [6].

In the late 1940s, a new anti-tumor drug, namely methotrexate, was discovered [6]. Injections of this chemotherapeutic agent limited the rapid growth of cancerous cells of acute lymphoblastic leukemia (especially in children) [6, 19]. It is currently being used to treat osteosarcomas (malignant tumors in the bones) and lymphomas [20]. Although this therapy was effective in controlling the tumor, it had the same problem of cyclophosphamide and cancer cells resistance was observed during the early stage of treatment [6].

Discovering and improving therapies to fight cancer did not stop and in 1962 another chemotherapeutic agent, 5-fluorouracil, was synthesized [6]. The agent was used in the treatment of colorectal cancer [21]. In the 1960s, a combination of cytotoxic therapies has been explored and specified for certain types of cancer including cisplatin which was researched as an antineoplastic agent in testicular cancer treatment [6].

Several cytotoxic drugs have been synthesized since the 1950s and 1960s [6] including Doxorubicin which is capable of treating osteogenic sarcoma, chronic myelogenous leukemia, Hodgkin's lymphoma and soft tissue sarcoma [22]. Although many chemicals were developed and helped in treating cancer, almost all had unwanted and often severe side effects on the normal healthy cells. In an attempt to overcome this drawback, Anti-hormonal cancer therapy was researched in the 1960s [6], with Tamoxifen being the first drug to be used clinically in the treatment of breast cancer in the 1980s. Then, other drugs were developed for breast and prostate tumors [6].

Over the past two decades and after understanding the nature and the interaction between anti-cancer drugs and the tumors, nanotechnology applications (including the development of nanocarriers) have been extensively researched to increase the specificity of anti-neoplastic agents towards cancerous tissues [13, 23-26]. Nanocarriers are developed to avoid some of the drawbacks of conventional chemotherapy including poor targetability, burst effects due to high doses and insufficient information about the drug disposition in the body (poor pharmacokinetics) [27]. These nanomaterials should be non-toxic, stable *in vitro* and *in vivo* environments, biodegradable and have controllable drug distribution and release [28].

There are two main mechanisms proposed to target anti-cancer drugs using nanocarriers: passive and ligand (also referred to as active) targeting [23]. The concept of the passive targeting is based on the leaky microvasculature of cancer cells allowing scientists to utilize the enhanced permeability and retention (EPR) effect to their advantage when designing new drug delivery systems [29]. The EPR effect was explained in 1986 by Maeda and coworkers when they discovered that larger molecules (with molecular weights greater than 40-50 kDa), such as proteins and polymers, accumulate effectively and are retained in cancer tissues for longer time compared to normal tissues [30, 31].

The EPR effect is behind many drug delivery therapies currently being researched to target tumors including liposomes, polyelectrolyte capsules, micelles and others [32]. The most important factor affecting the efficiency of the passive targeting of anti-cancer carriers is their particle sizes which should be in the range of 20-200 nm (to permeate through the gaps between the blood microvessels of malignant tissues) [29]. In addition, the extent of tumor microvasculature heterogeneity, which differs with the type of cancer and from one tissue in the tumor to another, may affect cellular uptake [33]. It is important to note that liposomal doxorubicin (Doxil and Myocet), and nanoparticle albumin-bound paclitaxel, both utilizing the EPR effect, are FDA approved for clinical use [29].

In ligand- or active- targeting, nanocarriers are functionalized by conjugating a ligand to their surface to target over-expressed receptors on the surface of

cancer cells [33]. Anti-cancer drug delivery carriers targeted "actively" and approved clinically include liposomal oxaliplatin conjugated using transferrin glycoproteins and immunoliposomal doxorubicin functionalized by human monoclonal antibodies (mAb), whereas several ligand-targeted therapeutics are currently in preclinical trials [29].

Among the recent nanoparticles investigated as effective drug carriers are metal organic frameworks (MOFs) [34]. Generally, MOFs have well-known crystalline structures with high surface areas that vary from 1,000 to 10,000 m^2/g, high porosity (the volume of pores may exceed 50% of the total volume). Additionally, they are formed and tuned from combining any metal ions with organic ligands to get different structures and sizes. This chemical and physical variability renders MOFs useful in many applications including activation of small molecules, gas storage and separation, catalysis of organic reactions and others [35].

In addition, some of MOFs have certain features that promote their use as drug carriers including nontoxicity, biocompatibility, ability to entrap high loadings of the drug (because of their porous nature) and small size [36]. Below, we review the methods used to synthesize MOFs and their recent use as anti-neoplastic drug delivery carriers.

2. LITERATURE REVIEW

2.1. History of Open-Framework Coordination

The first open-framework coordination was synthesized by Hofmann and Kspert in 1897 [37]. They prepared a hybrid network of $Ni(CN)_2(NH_3).C_6H_6$ crystals. After several decades, Pfeiffer and Feigl ended up with a 2-dimensional polymer consisting of one nickel molecule linked to two cyanide groups, ammonia and a benzene ring as shown in (Fig. **1**) [37].

In 1954, Powell and coworkers characterized $Ni(CN)_2(NH_3).C_6H_6$ using the X-ray diffraction (XRD) technique [37]. They found that the structure of the Hofmann model was not a 2-dimentional polymer. It is comprised of square flat Ni(II) metal centers surrounded by two cyano group $(CN)_2$ ligands, ammonia molecules and a benzene ring encapsulated inside these polymer sheets. Fig. (**2**) represents a partial structure of these network crystals [37].

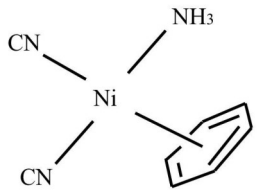

Fig. (1). The structure of the crystal developed by Pfeiffer and Feigl [37].

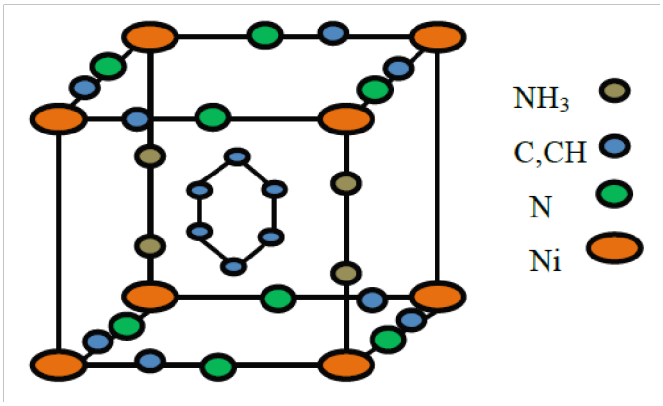

Fig. (2). A partial structure of the crystal developed by Powell and coworkers [37].

After that, several groups attempted to modify the Hoffman complex and synthesized different networks using different monomers with cyano group ligands and aromatic compounds. The structures of the resulting particles were determined (using XRD) to be crystals encapsulating the aromatic rings [37].

2.2. Methods for the Synthesis of the Metal Organic Frameworks

There are many routes to prepare MOFs with different structural designs. Most of them consist of metal clusters, bridging organic linkers and solvents while others are solvent-free. The metal salt and organic compounds can be mixed as solid powders in a solvent. Solutions of these solids can also be prepared first, and then mixed in the reactor [38]. The reaction occurs in the liquid phase after dissolving the reactants in the solvent which slows the reaction rate and absorbs the exothermic heat released [39]. Also, the solvent helps in forming the crystals thus obtaining the required MOF structure. Factors affecting the selection of a suitable solvent include: reactivity, solubility, its phase at the reaction conditions, phase spilt, association or dissociation constants, selectivity as well as its heating and cooling properties [40].

2.2.1. Low Evaporation Method

MOFs are usually synthesized using several steps. The first step is the precipitation reaction of the dissolved solids at room temperature. Then, crystals growth starts with the slow evaporation of the solvent. Although the low evaporation method does not require heat to evaporate the solvent, it is less efficient as it needs more time to complete compared to the other methods of synthesizing MOFs [38].

In 1989, Robson and coworkers designed the first organic network using an organic linker (instead of the CN group used in Hofmann complexes) [37]. They synthesized an infinite three-dimensional cationic MOF $\{Cu^{I}[C(C_6H_4.CN_4)]\}^{+}$ [41]. Firstly, a tetrabromo derivative, 4,4',4'',4-tetrabromotetraphenylmethane ($C_{25}H_{16}Br_4$), was prepared from 2.55 g of iron, 12.3 g of tetraphenylmethane ($C_{25}H_{20}$) and 29 g of Br_2 dissolved in 100 mL of CCl_4**.** Then, the resulting tetrabromo derivative was recrystallized in dimethylformamide (DMF) (xylene can also be used) and reacted with 0.97 g of CuCN in 2.6 mL of DMF**.** After 4 h, 4,4',4'',4-tetracyanotetraphenylmethane ($C_{29}H_{16}N_4$) was obtained by drying the mixture in vacuum at 100°C [41].

Amount of 22 mg of $[Cu(CH_3CN)_4BF_4^2]$ and 40 mg of $[C_{29}H_{16}N_4.½\ C_6H_6]$ were dissolved in a mixture of 1 mL of acetonitrile (CH_3CN) and 10 mL of nitrobenzene ($C_6H_5NO_2$). The solution was evaporated slowly and colorless crystals of $\{Cu^{I}[C(C_6H_4.CN_4]\ BF_4.[8.8C_6H_5NO_2]\}$ were obtained. Some of the crystals were collected, washed with nitrobenzene and dried in air. The remaining particles were kept in the main solution to investigate their morphology using the X-ray crystallographic analysis and found to be porous diamond-like shapes encapsulating random BF_4^- ions and nitrobenzene inside the cavities. Fig. (**3**) shows the structure of the MOF in which the larger circles represent the copper atoms, the rod-like units denote the organic linker ($C_{29}H_{16}N_4$) and the black lines denote a cavity with a volume of 700Å^3 (BF_4^- ions and $C_6H_5NO_2$ are not shown in the structure) [41].

Using this way, Robson and his group succeeded to design the first MOF and outlined a procedure to prepare porous solid polymers with well-defined sizes and shapes [41].

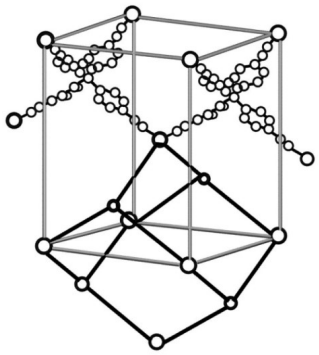

Fig. (3). The $\{Cu^{I}[C(C_6H_4.CN_4)]\}^{+}$ framework [41].

Another MOF was synthesized in 1994 from cadmium nitrate $[Cd(NO_3)_2]$ and 4,4' bipyridine (4,4'bpy) ($C_{10}H_8N_2$) that formed two-dimensional square framework with porous structure as shown in (Fig. **4**) [42]. To prepare this MOF, 2 mL of 4,4'-bpy (2.0 mmol) were dissolved in ethanol and 8 mL of aqueous cadmium nitrate (1.0 mmol) at room temperature and after 24 h, fine colorless crystals were collected [42].

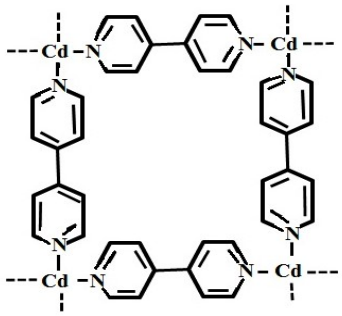

Fig. (4). The structure of $[Cd(4,4'\text{-}bpy)_2(NO_3)_2]$ [42].

The first attempt to encapsulate a material in the pores/cavities of $[Cd(4,4'\text{-}bpy)_2(NO_3)_2]$ was implemented to load o-dibromobenzene ($C_6H_4Br_2$). The encapsulation was confirmed by the XRD technique and the structure of loaded MOF was found to be a twodimensional graphite-like solid in two layers. Each layer comprises a planar square of cadmium ion and 4,4'-bpy at the edges and $C_6H_4Br_2$ in the empty spaces. Fig. (**5**) represents the structure of this complex [37].

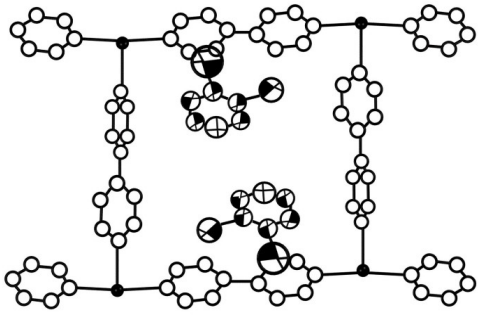

Fig. (5). The view of the complex $[Cd(bpy)_2](NO_3)_2(C_6H_4Br_2)_2$ [37].

2.2.2. Solvothermal Synthesis

Solvothermal synthesis is a chemical reaction in a solvent medium under subcritical conditions [43]. It is defined simply as any reaction occurring at elevated temperatures and constant pressure in a closed vessel, using organic or inorganic solvents. Diethylformamide (DEF), DMF, ethanol, methanol and acetone are the most commonly used solvents [38]. Factors affecting the solvothermal synthesis and the resultant MOF structure include temperature, concentrations of the reactants (metal salt and ligand), the ligand length and bond angles, the geometries, the solubility of the solids in the solvent and the pH of the liquid mixture [44]. When the metal salt is dissolved in water, the process is called hydrothermal synthesis [38].

In 1995, Zaworotko and coworkers prepared another organic coordination molecule $\{[Zn(4,4'bpy)_2]SiF_6\}$ that has square cavities with a volume of around 50% of the total volume [45]. First, 0.31 g of $[Zn(OH_2)_6]SiF$ were dispersed in 25 mL of benzene and 25 mL of 1,4-dioxane ($C_4H_8O_2$). The mixture was heated using the Dean-Stark apparatus to remove the water and obtain $ZnSiF_6$ as a powder. About 25 mL of DMF were added and the whole mixture was heated in a rotary evaporator where most of the 1,4-dioxane and benzene evaporated. The remaining mixture was cooled down and 0.31 g of 4.4'-bipyridine dissolved in 10 mL of 1,4-dioxane were added and heated for 30 min. Then, a yellow solution was observed and cooled at room temperature for 12 h, resulting in 0.48 g of colorless crystals of $\{[Zn(4,4'-bpy)_2]SiF_6\}$. The pores have a hydrophobic nature and thus can encapsulate hydrophobic materials only [45].

In the same year, Yaghi and his group researched the hydrothermal synthesis method and applied it to synthesize a new metal network $\{[Cu(4,4'bpy)_{1.5}]NO_3.(H_2O)_{1.25}\}$ [37]. They dissolved 0.17 g of $Cu(NO_3)_2.2.5H_2O$, 0.04 g of 1,3,5-triazine $(HCN)_3$ and 0.17 g of 4,4'-bpy in 15 mL of deionized water and poured the solution in a closed stainless steel bomb reactor and heated it in a furnace by increasing the temperature 5 degrees/min till it reached 140°C and then remained constant for 24 h [46].

Then, the resulting mixture was cooled gradually at a rate of 0.1 degree/min and when the temperature reached 90°C, it was kept constant for 12 h followed by cooling at the same rate to 70°C and held at the latter temperature for 12 h. Finally, it was cooled at a rate of 0.1 degree/min to the room temperature. The single-crystal XRD analysis showed the shape of the particles as three-dimensional porous networks consisting of copper atoms at the corners which are connected by rod-like bipyridine rings**.** The voids between the networks are filled with the water and nitrate ions [46].

2.2.3. Microwave-Assisted Irradiation Method

Microwave-assisted irradiation reduced the time required for crystallization at different ranges of temperature without any deformations in the MOF structure. However, it was not used frequently because not enough information was available about the crystals morphology to evaluate the structural data obtained for the nanoparticles [44].

In 2006, Z. Ni and R. I. Masel used this procedure to prepare three groups of MOFs, named IRMOF1 (zinc oxide with 1,4-benzenedicarboxylate), IRMOF2 (zinc oxide with 2-bromoterephthalic acid), and IRMOF3 (zinc oxide with 2-aminoterephthalic acid) [47]. The metal precursor and organic compound were dissolved in N,N-diethylformamide (DEF) and mixed for 15 minutes to get a homogenous solution. To synthesize IRMOF-1, 0.67 mmol of the metal precursor and 0.50 mmol of the organic linker were dissolved in 10 ml of DEF. One mL of the solution was poured into a closed Pyrex flask of 4 mL volume and placed in a laboratory microwave synthesizer. After 25 seconds, the product was centrifuged and IRMOF-1 microporous particles were collected. The crystals were characterized using scanning electron microscopy (SEM) and their shapes were found to be small cubes that had sizes ranging between 3-5 micrometers [47].

IRMOF-2 and IRMOF-3 were made using the same steps with different amounts of metal salt, ligand and solvent [47]. The microwave strategy is somewhat similar to the solvothermal reaction and the particles produced have the same quality, but the microwave requires less time [38].

2.2.4. Electrochemical Synthesis

Electrochemical synthesis was investigated in 2005 by researchers at Badische Anilin- & Soda-Fabrik (BASF) in Germany [48]. They tried to use metal ions instead of metal salts to reduce the cost for large scale MOF production. As a result of oxidation and reduction, hydrogen gas was formed and the metal ions were deposited on the cathode [48].

Protic solvents including methanol, ethanol and isopropanol can be used to remove the deposited metal [48]. An example of MOF prepared by the electrochemical methods is $Cu_3(BTC)_2$ prepared from zinc oxide and 1,3,5-benzenetricarboxylic acid (BTC).

When the metal was immersed in the electrolyte solution containing the organic ligand and a salt of methyltributylammonium methyl sulfate (MTBS), the electric voltage was produced and crystals of $Cu_3(BTC)_2$ grew due to the electrochemical reaction. XRD was used to determine the size of the particles which were found to be in the range of 2 to 50 μm [49].

2.2.5. Mechanochemical Synthesis

Recent studies reported this route as a solvent-free process that depends on a mechanical force to induce the chemical reaction that produces MOFs. Grinding the solid substances produces mechanical energy that breaks the bonds of the solids allowing the chemical reaction to take place, thus forming other intermolecular bonds of the produced crystals. Although this process is carried out without a solvent, a small amount of solvent is used with the solid mixture to aid in the grinding step, and thus the reaction proceeds at a faster rate [38].

M. Klimakow *et al.* synthesized two MOFs from copper acetate monohydrate cluster with BTC and the same cluster with 4,4',4''-benzenetribenzoic acid (H_3BTB) in ethanol [50]. The mixtures were prepared in a molar ratio of 3:2 and grinded for 25 minutes in a conventional ball mill. The resulting MOF structures are shown in (Figs. **6** and **7**) [50].

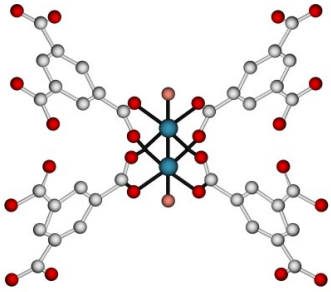

Fig. (6). The H_3BTC metal organic framework [50].

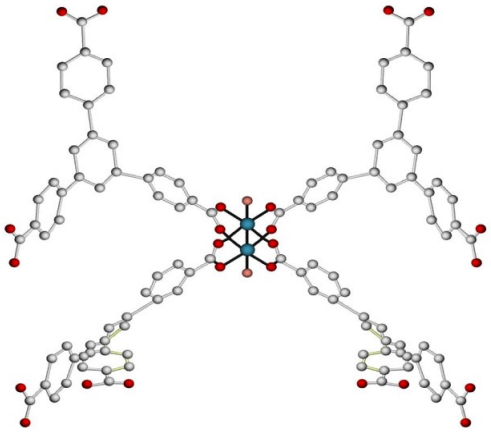

Fig. (7). The H_3BTB metal organic framework [50].

2.2.6. Sonochemical Synthesis

The routes of preparing MOFs have been developed to reduce the time of crystallization and get homogenous particle structures. Sonochemical synthesis is a rapid method in which high-energy ultrasound radiation is used as a driving force for the chemical reaction to produce micro- or nanoMOFs. The ultrasonic waves are cyclic mechanical vibrations that have frequencies above 20 kHz [38]. When applied, they stimulate the reactant molecules to move rapidly and strike each other. As a result of the cyclic vibrations, bubbles start to grow in the liquid mixture of the metal salt, ligand and solvent. The size of these bubbles increases until they collapse and release their energy producing high temperatures and pressures in the process [38]. Due to the differences in the pressure and temperature of the new bubbles formed and the reaction mixture, MOF crystals grow quickly [51].

The first MOF prepared by the sonochemical procedure was synthesized from BTC and an aqueous solution of zinc acetate salt. The reactants were added into a mixture of water and ethanol and sonicated for a short time (less than 30 min). The produced particles ($Zn_3(BTC)_2$) had spherical structures with sizes ranging between 100-200 nm. When the reaction time was increased to 30 and 90 min, the resulting MOFs looked like long needles with larger diameters (up to 900 nm) [48].

Sonochemical synthesis was applied to construct many other MOF networks including MOF-5 (Zn_4O nodes with 1,4-benzodicarboxylic acid), Fe-MIL-53 [$FeCl_3.6H_2O$ with terephthalic acid(BDC)] and HKUST-1 (copper nodes with BTC). This synthetic approach is environmentally friendly and effective in terms of the cost and energy (the reaction occurs at room

temperature using ultrasonic irradiation). In addition, it can produce high yields of homogeneous nanocrystals in a shorter time compared with the other synthesis routes [48].

Using different metal salts and organic ligands, unlimited structures can be formed and used for different applications.

2.3 The First MOFs as Potential Drug Carriers

The first family of MOFs that can be used in drug delivery systems was investigated in 2006 by Horcajada and co-workers [52]. It consists of two groups called MIL-100 and MIL-101 (MIL is abbreviation of Materials of Institut Lavoisier). These two examples were synthesized using carboxylic acid groups as organic ligands and trivalent metals as clusters. The MIL family has many structural characteristics that promote its use as drug carriers including large pores (with identified surface areas) and its ability to form a hybrid network [52].

Horcajada and co-workers carried out experiments to study the kinetics of the Ibuprofen (antiinflammatory drug) loading and release using MIL-100 and MIL-101 complexes with chromium (Cr) [52]. MIL-100 was synthesized by mixing metallic chromium, BTC, hydrofluoric acid (HF) and water with a molar ratio of 1: 0.67: 1: 265. Then, the mixture was placed in a Teflon-lined bomb and heated gradually for 4 days at 220°C. The other MOF, MIL-101, was synthesized by heating a mixture of chromium (III) nitrate [$Cr(NO_3)_3 \cdot 9H_2O$], HF, BDC and water in a molar ratio 1: 1: 1.5: 280 for 10 h at 220°C in a Teflon-lined bomb reactor/ calorimeter. To collect the particles, the mixture was cooled down, filtered and dried at 100°C in an oven for 24 h. Fig. (**8**) shows the structure of Cr-MIL100 and Cr-MIL-101 [52].

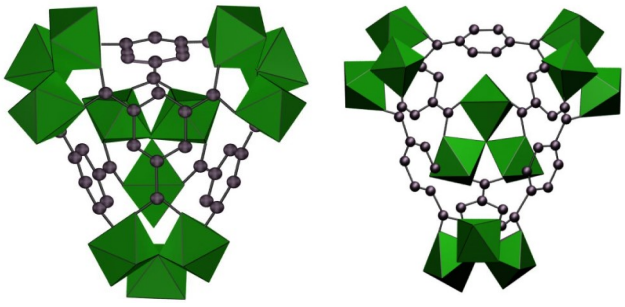

Fig. (8). The Cr-MIL-100 (left) and Cr-MIL-101 (right) structures [52].

The loading was carried out by dissolving 100 mg of MIL-100 and 100 mg of MIL-101 in 10 mL of hexane and stirring in the presence of 200 and 400 mg ibuprofen, respectively. Ultraviolet-visible (UV-Vis) spectroscopy showed loading to be 0.35 g Ibuprofen/g MIL-100 and 1.4 g Ibuprofen/g MIL-101. Although the loadings of the carriers were relatively high, they did not affect the structure of the MOF when characterized by XRD. Then, Ibuprofen release was observed and controlled under certain conditions and occurred completely within three and six days for MIL-100 and MIL-101, respectively, which was slow enough to reduce the side effects usually experienced by a patient taking the medication [52].

To investigate the release kinetics, 200 mg of the encapsulated drug was compressed by applying an isostatic pressure of 3 MPa and uniaxial pressure of 2.75 MPa. 13-mm Diameter Discs were obtained and impregnated in a stimulated body fluid (SBF) at 37°C. High performance liquid chromatography (HPLC) was used to determine the concentration of the drug released in the SBF. It was found that the entire release from MIL-100 took 3 days, and it took 6 days in the case of MIL-101. Despite the efficiency of this administration route, the particles were synthesized using chromium which is toxic. Therefore, its application in drug delivery is restricted. Toxic chromium can be replaced by other metal ions including iron, copper, manganese, zinc and nickel which are nontoxic and are naturally found in the body [52].

Generally, the MIL constructs are hydrophobic polymers that are suitable for encapsulating hydrophilic drugs [53]. However, there are other MOFs with hydrophilic pores used to deliver cationic drugs. Lately, Rosi and coworkers succeeded in preparing a new MOF (bio-MOF-1) based on one of the purine derivatives, namely adenine ($C_5H_5N_5$), and zinc (II) ions and used it to encapsulate procainamide (antiarrhythmic drug) [54]. The MOF was prepared by dissolving 0.125 mmol of adenine, 0.375 mmol of zinc acetate dihydrate [$Zn(CH_3COO)_2 \cdot 2H_2O$] and 1 mmol of nitric acid in 1 mL of water and 13.5 mL of DMF. The mixture was placed in a capped vial and heated at 130°C for 24 h. Then, the resulting crystals were collected, washed 3 times with 3 mL DMF and dried for 30 min under argon [54].

To determine the drug loading, about 0.914 g of the MOF was soaked twice in an aqueous solution of 0.1 M of procainamide hydrochloride for 10 min and the solution was removed. Then, the impregnation was carried out for 24 h followed by solution removal. This

procedure was repeated every 24 h and after 15 days, the final loading was found to be 0.22 g of procainamide inside the MOF/g procainamide added to the MOF. The release was then investigated by adding 15 mg of the loaded drug to 0.1 M phosphate buffered saline (PBS) [54]. PBS is used in biological research because its ion concentrations match those of the human body [55]. 100% release was observed by HPLC and occurred after three days. When the complexes were loaded in nanopure water (not PBS), the release was only 20% of the amount inside the framework, indicating that the main reason for the release was the cations in the saline solution [54].

As there are unlimited numbers of MOFs that can be synthesized, they should be selected carefully when used for medical applications. The toxicity and stability levels should be examined before their use.

2.4. MOFs as Anti-Cancer Drug Carriers

Recently, metal organic frameworks have attracted attention as anti-cancer drug carriers, because of their low toxicity and high efficiency [56]. In 2009, Lin and coworkers reported the loading of cisplatin in the nanoporous MOF, MIL-101 (Fe) [57]. Cisplatin and its derivatives are targeted anti-cancer therapies based on platinum metal and used effectively to cure testicular and ovarian cancer, but their level of toxicity can cause severe side-effects including nausea, nephrotoxicity and bone marrow suppression [58]. To reduce the unwanted side effects, one of the cisplatin derivatives, ethoxysuccinato-cisplatin (ESCP), which treats carcinomas including cancers of soft tissue, bones, muscles, sarcoma cancers and blood vessels [59], was loaded in a functionalized Fe-MIL-101 [57].

To synthesize the functionalized Fe-MIL-101, typical amounts of 1.38381 mmol of $FeCl_3 \cdot H_2O$ and 1.38381 mmol containing 17.5 mole% 2aminoterephthalic acid (NH_2-BDC) [$H_2NC_6H_3$-1,4$(CO_2H)_2$] and 82.5% BDC were dissolved in 30 mL of DMF and heated to 150 °C for 15 min in a sealed microwave vessel using a HP500 microwave. The resulting mixture, which contained the particles, was then cooled down at ambient temperature and centrifuged. The particles were collected and washed with ethanol and DMF to remove the excess reactants. Experiments showed that 17.4 mol % NH_2-BDC incorporated with the metal to form the MOF [57].

The loading of the drug was carried out in two steps. First, 22 mg of ESCP and 9.3 mg of 1,1carbonyldiimidazole [$(C_3H_3N_2)_2CO$] were dissolved in 3 mL of DMF and heated, under argon, at 60 °C for 1 hour followed by cooling to room temperature. The purpose of adding 1,1-carbonyldiimidazole is to activate the cisplatin. Then, 85 mg of the MIL-101 (Fe) was stirred with the solution at room temperature for 48 h and the loaded particles were collected by centrifugation and washed with ethanol and DMF. The washed particles were isolated from the solution by dialysis using distilled water as a buffer for 5 hours (the water was changed every hour) [57].

The collected particles had the same structure asMIL-101 with the same diameter (200 nm) and loaded 12.8 wt% of the drug. In addition, the release was measured using a spectrofluorometer completed after 1.2 h in PBS at 37°C. Experiments revealed that the MOF particles were not stable and decomposed in the buffer solution; therefore the loaded nanocarriers were coated by a thin layer of sodium metasilicate (Na_2SiO_3) to slow down the release [57].

The Fe-MIL-101 nanoparticles were coated with sodium silicate as follows: 10 mg of the loaded nanoparticles were suspended in ethanol, centrifuged and then dispersed in 4 mL of water. Then, 47.5 mg of sodium silicate ($Na_2SiO_3.5H_2O$) were dissolved in 2 mL of water and HCl was added to neutralize the solution. This solution was added to the nanoparticles suspension and the entire mixture was diluted to 20 mL by adding water. The resulting suspension was stirred at 60°C for 3 h followed by centrifugation. The coated particles were washed with ethanol and water, and dispersed in ethanol for further experiments. The release through the silica shell took 14 hours instead of 1.2 hour under the same conditions. When the coated nanoparticles were used against colon cancer (HT-29) cells, it showed lower cytotoxicity and induced more cells death compared to cisplatin [57].

The loaded drug was activated and modified to target specific tumor cells in two ways. First, glutathione antioxidant ($C_{10}H_{17}N_3O_6S$) was used to activate the content of the silica shell inside the cells. Second, the MOF was functionalized by attaching a cyclic peptide ($C_{27}H_{41}N_9O_7$) called c(RGDfK), the latter having an affinity towards $\alpha_v\beta_3$ integrin receptors found in many cancer cells. Fig. (**9**) represents the scheme of the previous steps [57].

To attach the peptide, the coated nanoparticles (cisplatin loaded in Fe-MIL101) were dispersed in ethanol with a concentration of 2 mg/mL and the

c(RGDfK) solution was added to the suspension. The mixture was diluted by adding aqueous HCl to obtain a pH of 3 and then stirred for 1 day in the dark to conjugate the c(RGDfK). The targeted particles were centrifuged, washed with and dispersed in ethanol. HT-29 human colon adenocarcinoma cells (ATC # HTB 28) were targeted efficiently using the new modified therapy with cytotoxicity (IC_{50}=21 μM) similar to that observed with free cisplatin [54, 57].

The highly porous synthesized MOF (MIL-101) succeeded in encapsulating the cisplatin derivative (ESCP) with 12.8 wt% payload and the release was prolonged by coating the particles. The release was completed after 12 h [57].

Another reported chemotherapeutic agent loaded in nanoMOFs is topotecan (TPT), a member of the cytotoxic drug family camptothecin (CPT). It is a hydrophobic drug that dissolves slightly in water and is used to treat lung, cervical and ovarian tumors. The drawbacks of using TPT include the high toxicity of the carboxylate form and its low cellular uptake. These challenges were tackled by loading the drug in different nanocarriers including MOFs. Results of loading the chemotherapeutic inside carriers showed a decrease in toxicity and an increase the amount of TPT taken up by the cells [60, 61].

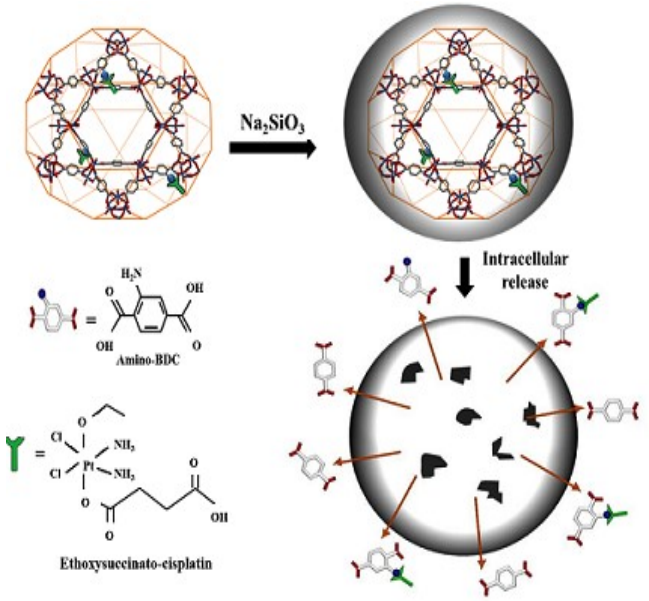

Fig. (9). Attachment of ethoxysuccinato-cisplatin through amino groups on NH2-BDC particles [57].

TPT was loaded in porous Fe-MIL-100 to control the release. The MOF was prepared by the hydrothermal method via microwave heating. A mixture of 8.97 mmol of iron(III) chloride and 4.02 mmol of trimesic acid [$C_6H_3(CO_2H)_3$] in 20 mL of demineralized water was heated to 130°C for 6 minutes under stirring all while applying 400 W of microwave power (to reduce the crystallization time). Then, the mixture was centrifuged for 10 min at 10,000*g to separate the nanoparticles. The particles were later washed with 50 mL of ethanol and recovered by centrifugation [61].

Aqueous solutions of the drug with 0.004, 0.04, 0.14, 0.42 and 2.05 mM concentrations were prepared. The loading was carried out by incubating 3 mg of the MIL-100 in 4.5 mL of the TPT solution and the mixture was divided into 3 microcentrifuge tubes of 1.5 mL. They were stirred for 24 h at room temperature and the loaded nanoparticles were separated from the water by centrifugation for 10 min at 10,000*g. Then, they were washed 3 times with water and kept at 22 °C under vacuum for 24 h. A general scheme of the loading is shown in (Fig. **10**) [61]. The percent of the drug encapsulated in the MOFs (by weight) at the five concentrations were determined by an UV-visible reflectance spectrum and found to be approximately 0.14, 1.3, 4.0, 5.6 and 33 wt %, respectively [61].

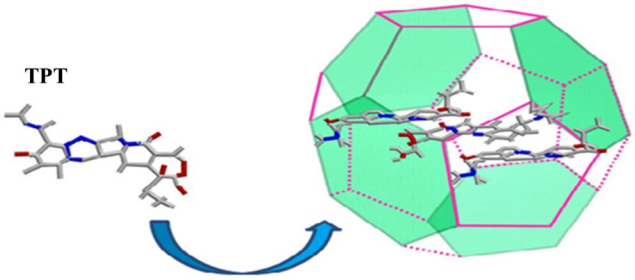

Fig. (10). The scheme of entrapping TPT within MIL-100 nanoMOFs [61].

Another aqueous solution of the drug (0.023 mM) was prepared and the loading was achieved using seven successive impregnations. Two mg of MIL-100 were added to 9 mL of the drug solution and kept at room temperature for one day. After that, the loaded MOFs were centrifuged for 10 min at 10,000*g and washed with water. These steps were repeated seven times using fresh TPT solution in each impregnation and the resulting nanoparticles were kept at 22°C under vacuum for 24 h. The cumulative loading percent (after the last incubation) was 11.6 wt% [61].

For the highest loading, 33 wt%, the transmission electron microscopy (TEM) technique confirmed that the nanoparticles had the same size distribution and structure before and after the drug encapsulation. The

diameter range of most of these nanocarriers varied between 50 and 150 nm, whereas few of them were larger (their sizes ranging between 200 and 400 nm) [61].

The release was investigated for different loading percentages (1.4, 11.6 and 33 wt %) in two media (water at pH ~ 6.7 and PBS at pH ~ 7.4) at 37°C with and without photon irradiation. In water, after 24 h of incubation, the fluorescence detected that 5.0 and 4.0 % of the drug was released from the first two loadings, respectively, whereas the highest loading (33 wt%) did not show significant release (it was only 0.005%). When one photon irradiation has been applied for the three payloads, the release was increased to 9.0, 13, and 2.5%, consecutively [61].

In addition, two-photon irradiation was applied for the 11.6 and 33 wt % loadings and the corresponding release percentages were determined to be 28 and 2.8%. On the other hand, after 24 h of incubation in PBS, the lowest loading showed the fastest release. Around 60% of the loaded TPT was released within the first hour and 93% after 24 h [61]. The phenomenon of releasing higher amounts of the drug initially (as was the case at the 1.4 wt% payload) within a short period is called burst release which reduces the targeting of the drug to the tumor cells and increases the toxicity level [62]. The release percent for the 11.6 and 33 wt% payloads were detected after 26 h of incubation and found to be around 40 and 15%, respectively [61].

The *in vitro* study of 11.6% loaded nanoMOFs was performed using human MiaPaCa-2 (lung carcinoma), PANC1 and A549 (pancreatic cancer) cell lines. Free TPT was incubated with the three cell lines for 72 h and IC_{50} was found to be 0.4, 1.6 and greater than 25 μM for MiaPaCa-2, A549 and PANC1, respectively, whereas the encapsulated drug showed different results (0.2, 2.5 and 2.4 μM, respectively). The group concluded that using the loaded drug increases its effectiveness against both PANC1 and MiaPaCa-2 cells while it decreases in the case of the A549 cell line [61].

Encapsulating the hydrophobic drug, TPT, in MIL100 improved the loading efficiency of the drug in the carrier as it reached 33 wt% compared to 0.6, 5.5 and 6.2 wt% when liposomes, solid lipid nanoparticles and nanostructured lipid nanocarriers were used, respectively. The same study proved that applying one- and two-photon light irradiation technique represents a viable approach to trigger the release of TPT in a controlled manner [61].

Busulfan is a chemotherapeutic agent used in high doses to treat chronic myelogenous leukemia [63] and osteosarcoma [64]. The strategy of encapsulating this drug in porous MOFs was two-fold: to avoid its degradation in aqueous solutions and prohibit its accumulation in the liver [65]. Four MOFs (MIL-88A, MIL-89, MIL-53 and MIL-100) were synthesized, then the drug was loaded in the MOFs through mixing and the release and loading were measured. MIL-88A was synthesized by heating 10 mL of iron chloride hexahydrate ($FeCl_3.6H_2O$) and 10 mmol/L of fumaric acid ($C_4H_4O_4$) while being mixed for two min at 80°C (with 600 W microwave power applied to assist in the heating). The second MOF (MIL-89) was obtained when 1 mmol of iron acetate ($C_{14}H_{27}Fe_3O_{18}$) was mixed with 1 mmol of trans,trans-muconic acid ($C_6H_6O_4$) and dissolved in 5 mL of methanol and 0.25 mL sodium hydroxide. The liquid mixture was heated for 6 hours in a Teflon-lined steel autoclave at 100°C [65].

The third MOF (MIL-53) was prepared solvothermally by heating a mixture of 1 mmol of $FeCl_3.6H_2O$ with 1 mmol of BDC [$C_6H_4(CO_2H)_2$] and 5 mL of DMF at 150°C for 2 h. Finally, MIL-100 was obtained by mixing 8 mmol of aqueous iron ion, 5.3 mmol of BTC, 4 mmol of hydrogen fluoride and 40 mL of water. Then, the mixture was placed in a pressure chamber and heated under microwave irradiation for 30 min until it reached 200°C After that, the four mixtures were centrifuged for 10 min at 5,600*g and washed with 100 mL of deionized water to obtain MIL-88A and 100 mL of ethanol to obtain MIL-89, MIL-53 and MIL-100. Then they were centrifuged for a second time and dried at room temperature. MIL-88A and MIL-89 had faceted structures with sizes ranging between around 100 ± 25 and 75 ± 25 nm, respectively, whereas MIL-100 and MIL-53 represented trigonal shapes with mean diameters of 100 ± 50 and 350 ± 100 nm, respectively [65].

To carry out the loading of busulfan in the prepared MOFs, two solutions of the drug were prepared using dichloromethane and acetonitrile solvents to obtain final concentrations of 10 and 30 mg/mL, respectively. Then, 25 mg of the final MOFs produced were dehydrated at high temperatures, suspended in 2.5 mL busulfan solutions and stirred for 16 hours. The loaded particles were recovered by centrifugation for 10 min at 5,600*g and kept at room temperature under vacuum for 72 h.

After that, 20 mg of MIL-53 and MIL-100 nanoparticles were incubated in 2 mL of the drug solution (10 mg/mL of busulfan solution in dichloromethane) and 1 μL of acetonitrile for 24 h at room temperature under stirring. The nanoparticles were separated (using the same procedure mentioned above) and the loading percentages were determined by NMR spectroscopy and found to be around 13 and 25 wt% for MIL-53 and MIL-100, respectively. Elemental analysis was then implemented on the dried loaded four MOFs and the payloads were approximately 8, 14, 10 and 26 wt% for the MIL-88A MIL-53 MIL-89
MIL-100, respectively [65].

The release was investigated for MIL-100 and MIL53 at pH 7.4 by suspending 25 mg of the encapsulated busulfan in PBS at 37°C under stirring for several time durations and centrifugation at 5,600*g for 10 min. For each experiment, 1 mL of the solution was replaced with fresh PBS. The release of the encapsulated drug (in PBS) was 38% in the case of MIL-53 and 61% for MIL-100 during the first 30 minutes. After 2 h, the release increased to 58% and 76%, respectively, whereas the remaining portion was released within 6 h. Additionally, some *in vitro* experiments were carried out on human multiple myeloma (RPMI-8226), human leukemia (CCRF-CEM) and human macrophages
(J774) cell lines to compare the cytotoxicity of free and loaded busulfan in MIL-100. After incubating the nanoparticles with cells for 48 h, the loaded drug showed similar results of cytotoxicity compared to the free drug [65].

Another application of MOFs as anti-cancer drug carriers attempted to load doxorubicin (DOX) in MIL100(Fe) [27]. DOX is a cytotoxic anti-cancer agent used frequently for childhood solid tumors, breast cancer, soft tissue sarcomas, myeloblastic leukemias and lymphomas [66]. Although it is used widely, it has adverse side effects including vomiting, nausea, hair loss, necrosis and oral mucositis, all of which limit its use [67]. The three main issues related to DOX's use in cancer treatment clinics are: cardiotoxicity during the first two or three days of its use [68] which causes congestive heart failure and heart muscle disease (cardiomyopathy) [69], its tendency to self-assemble in aqueous solutions that limits the amount of the drug taken by the cells and the cancer cells resistance is observed after a short therapy period [70].

To overcome the above mentioned disadvantages DOX, it was loaded in MIL-100(Fe) which was synthesized using the same procedure as TPT described above (6.0 mmol of iron(III) chloride was used instead of 8.97 mmol). Five mg of the MOF were added to 1.5 mL of aqueous DOX (10 mg/mL) and stirred for 24 h. To increase the loading, the incubation was repeated twice and then the loaded particles were separated by centrifugation at 5,600*g for 15 min and left to dry for 3 days under vacuum. The loading was investigated by an UV−visible absorption spectrum and found to be 9.0 wt%. The release was also studied using 5 mg of the encapsulated drug in 2 mL of PBS at pH 7.4 [24]. The drug release study showed fast release kinetics and reached 25% in the first 12 h, and then took 13.5 days to reach 100% release. Fig. (**11**) shows the structure of DOX-MIL-100(Fe) [27].

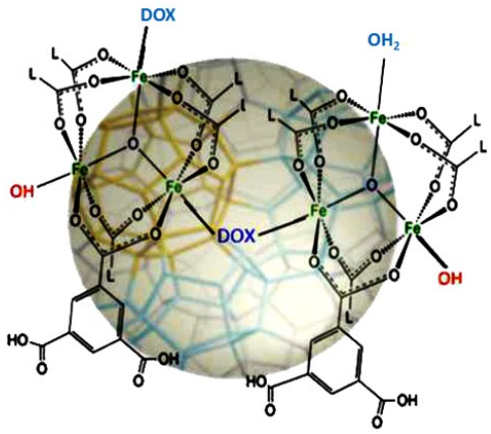

Fig. (11). A schematic of MIL-100(Fe) with DOX [27].

This example confirms the efficacy of using MIL100 as a good candidate for encapsulating anti-cancer drugs with relatively high loadings and controlling the release in time and space [27].

Zeolitic imidazole frameworks (ZIFs) are another example of MOFs synthesized using zinc salts and imidazole organic compounds and used in drug delivery. One compound that belongs to this category, ZIF8, was synthesized by mixing 330 mg of 2-methyl imidazole ($C_4H_6N_2$) with 150 mg of zinc nitrate hexahydrate [$(Zn(NO_3)_2.6H_2O$] after dissolving each one in 7.15 mL of methanol. The mixtures were prepared in a glass container and 2 mg/mL fluorescein (model drug) was dissolved in methanol and added to the zinc precursor. Then, the solution of 2-methyl imidazole was poured into the zinc and fluorescein concoction and stirred for 5 min. The solution changed in color (turned milky), indicating the progression of the reaction and hence the formation of the loaded nanoparticles [71].

The nanoparticles were separated from the solution by centrifugation at 7,000 rpm for 10 min and then washed three times with 10 mL of methanol to remove any remaining unreacted materials. The encapsulated fluorescein had a yellow color and was stored as a suspension in 5 mL methanol for further use. The resulting nanospheres had a porous crystalline structure and their average size was approximately 70 nm. Their sizes are identical to those for the MOFs before loading the fluorescein. Fig. (**12**) shows the loading of fluorescein molecules in ZIF-8 [71].

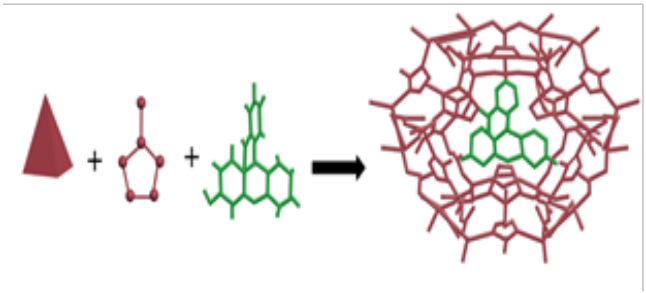

Fig. (12). A schematic of Fluorescein encapsulated inside ZIF-8 frameworks [71].

Different amounts of fluorescein were loaded inside the ZIF-8 nanoparticles with a maximum loading of 1 wt. Then, the stability of the nanoparticles was examined in a PBS solution and their structures remained intact at neutral pH and after 24 hours less than 10% of model drug was released. The low percentage of release was improved by lowering the pH (using an acidic buffer) and reached 50% after one hour. The loaded drug was then used in the treatment of MCF-7

breast cancer cells. The particles were capped with cetyltrimethylammonium bromide (CTAB) and incubated with the cells for 12 hours. The median effective dose (ED_{50}) was found to be45µg/mL, which is in the same range as that exhibited by the mesoporous silica nanomaterials and other MOFs [71].

5-Fluorouracil (5-FU) is another anti-cancer drug loaded in ZIF-8 [72]. The anti-neoplastic agent is used to treat various cancers including liver, breast, brain, gastrointestinal tract, pancreas and other solid tumors. The hematological, gastrointestinal and dermatological side effects of this cytotoxic drug limit its clinical applications, thus it was encapsulated in ZIF-8 to overcome these drawbacks [73]. The MOF was prepared by the procedure reported by Yaghi and co-workers [72]. Typical amounts of 0.21 g of $Zn(NO_3)_2.4H_2O$ and 0.06 g of 2-methyl imidazole were dissolved in 18 mL of DMF in a capped vial. The mixture was heated in a programmable oven gradually (at a rate of 5°C/min) to 140°C for 24 h followed by cooling (at a rate of 0.4°C/min) to room temperature. After that, the mother solution was removed and 20 mL of chloroform were added. The produced particles were collected, washed with 10 mL of DMF and left to dry in air for 10 min [72, 74].

The drug loading study was performed by drying 20 mg of ZIF-8 in tan oven at 160°C for 24 h and then stirring in a solution of 5 mL of methanol containing 30 mg of 5-fluorouracil for 2 days. The resulting solution was dried overnight at 50°C and the loading determined using an UV–visible absorption spectroscopy and found to be 660 mg of 5-FU/g of ZIF-8. The release was measured at 37°C by a fluorescence spectrophotometer in two media, acetate buffer (pH 5.0) and PBS (pH 7.4). In PBS, 50% of the loaded 5-FU was released at the early stage (after around 10 h) and the remaining encapsulated drug showed slow release which reaching approximately 85% after 7 days [72].

The release of 5-FU from ZIF-8 nanocarriers increased remarkably in acetate buffer and reached approximately 45% in 1 h, while only 17% was released in PBS within the same timeframe. After 12 h, the release plateaued at 85%. The study concluded that, the rate of release of 5-FU from ZIF-8 is faster in acidic medium (tumor tissues) than in blood circulation (neutral environment) [72].

Another chemotherapeutic drug, Camptothecin (CPT), was loaded in ZIF-8 using the above mentioned procedure by adding 1 mg of the agent. As is the case with other anti-neoplastic agents, this drug was encapsulated in the MOFs to reduce its unwanted side effects. The loading of CPT molecules in ZIF-8 is shown in (Fig. **13**) [71].

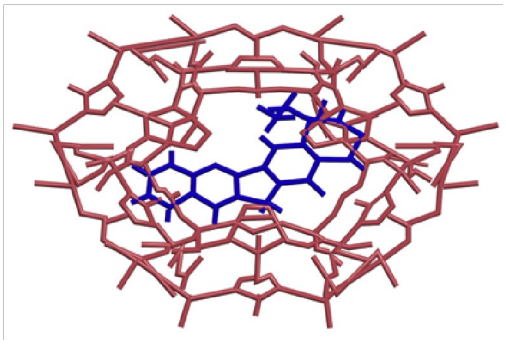

Fig. (13). A schematic of Camptothecin encapsulated inside ZIF-8 frameworks [71].

The maximum loading obtained was 2 wt % and the EC_{50} was found to be 22 µg/mL**.** After preparing the loaded drug, it was incubated with MCF-7 cells for 24

hours and the results showed that using CPT-ZIF-8 has induced more cell death compared with those treated with free CPT. Additionally, it was shown that ZIF-8 attracts only molecules with negative charges, including camptothecin and fluorescein, and lower of encapsulation was measured when positively charged molecules were used [71].

In another study, DOX was incorporated in ZIF-8

particles. The MOF was synthesized by mixing 0.6 g of zinc nitrate hexahydrate salt dissolved in 10 mL of methanol in a scintillation vial and 1.3 g of 2-methyl imidazole dissolved in 10 mL of methanol in another vial. The organic linker solution was added to the metal precursor and stirred for 30 min. Then, the nanospheres were centrifuged, washed 5 times with methanol, placed in an oven at 100°C to dry, and kept at room temperature to load the drug. ZIFs-8 and DOX are positively charged, so the procedure used to encapsulate fluorescein and camptothecin cannot be followed which dictated the use of another loading technique. The drug was dissolved in methanol and mixed with 100 mg of ZIFs and stirred for 2 days. The DOXZIFs particles were collected by centrifugation, washed with methanol several times, and dried [75].

The percentage of DOX loaded inside the MOF was found to be 52% of the initial amount used in the preparation experiments. ZIF-8 is stable at neutral pH and starts to dissociate in acidic solutions, so the release was expected to occur in the more acidic environment of the cancer cells is acidic, whereas the pH of the normal cells is around 7.4 and at this pH the release is considerably slower. The release was measured for 2.5 h at pH 5, 6, and 7.4, and results showed the rate decreased with increasing pH. A simple scheme representing the encapsulation of DOX into ZIF-8 is shown in (Fig. **14**) [75]**.**

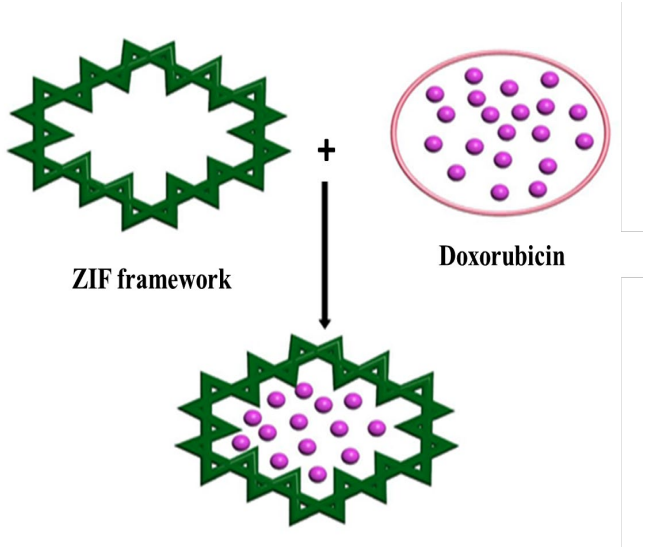

Fig. (14). A schematic of doxorubicin encapsulation inside ZIF-8 framework [75].

The nanospheres used in the examples above showed ZIF-8 as the first pH-sensitive MOF that can utilize the acidic environment of the tumor to release its contents [71, 75].

DOX was successfully encapsulated in another MOF that was prepared from gadolinium (III) salt and 1,4-bis(5-carboxy-1H-benzimidazole-2-yl)benzene)) linker (pDBI). First, 0.02 g of pDBI was dissolved in 1.5 mL of DMF and added to a 2.5-mL $Gd(NO_3)_3.6H_2O$ solution (0.023 g). Then, the aqueous mixture was sonicated for 10 min in an ultrasound bath, then heated at 110°C for 3 days in a closed vial and the crystals were collected. Fig. (**15**) shows the linker rotamers and space-filling model of Gd-pDBI [76].

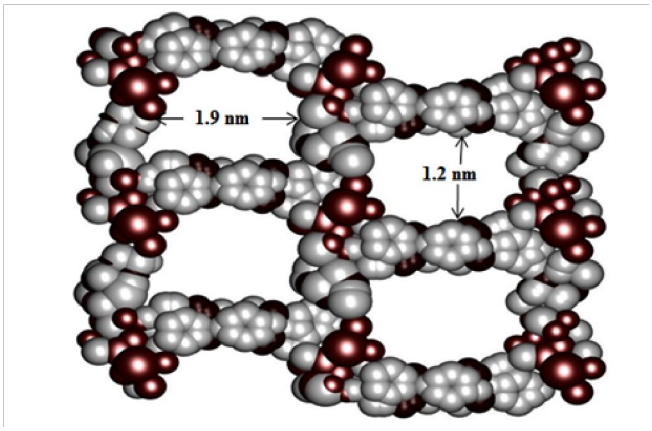

Fig. (15). A representation of the linker rotamers and spacefilling model of Gd-pDBI along the a-axis [76].

The synthesized Gd-pDBI (50 mg) was grinded by a ball milling machine for 30 min to downsize the particles from 0.5 mm to 120 nm (to produce MG-GdpDBI) and then used to encapsulate DOX. The

loading was done by sonicating the MOF particles added to 5 mL of Milli-Q (ultrapure) water. Two mg of DOX were dissolved in 1 mL Milli-Q water, added to the Gd-pDBI solution and sonicated for 5 min [76].

The mixture was left under stirring in the dark for one day to get MG-Gd-pDBI-DOX. The loaded drug was centrifuged at 12,000 rpm for 15 min followed by washing it twice with abundant Milli-Q water. The DOX concentration was varied from 0.33 to 2 mg/mL and the loading was found to be 5 wt% and 12 wt%, respectively. The release was then studied in two different environments (pH 7.4 and 5) using 5 mg of the loaded drug in 3 mL of buffer solution [76].

At pH 5, 44% of the DOX was released from GdpDBI (5 wt% loaded) in 5 days. The release became insignificant after 4 h, whereas only 22% of the antineoplastic agent was released at neutral pH. This result insures that the effect of the anti-cancer drug on healthy cells will be less pronounced compared to its effect on cancerous tissue, and hence the side effects of chemotherapy might decrease. Both *in vitro* and *in vivo* experiments were conducted to measure the efficiency of MG-Gd-pDBI-DOX as a drug delivery system (DDS). A model cell line (namely U 937- a human leukemia cancer cell line) was incubated for 2 days with the MOF to examine the *in vitro* anti-cancer activity and 50% of the cancer cells were inhibited at a DOX concentration of 75 mg/mL [76].

Further experiments were carried out and confirmed that the MG-Gd-pDBI is stable and biocompatible in the blood/blood plasma. The study showed that every Gd-linker contained two DMF molecules, an undesirable finding since DMF is toxic and may precipitate in the liver [77]. Hence, another set of experiments were conducted to evaluate the *in vivo* toxicity of MG-GdpDBI on healthy young (8-weeks old) Swiss albino mice. Using the same concentration as above, the mice injected with suspended MG-Gd-pDBI in water did not show any serious health problems or an increase in mortality rate [76].

Additionally, the blood and serum biochemical components were not affected by the MOFs and their values were the same as for the non-injected mice. Also, the kidney regulators and other parameter including the total phosphorous and protein contents remained unchanged. The functions of the other organs including heart, brain, spleen and lung were not affected in both treated and normal murine and the only minor health deterioration was found in the liver where some of the MG-Gd-pDBI accumulated/precipitated [76]. The study concluded that, encapsulating DOX in MG-Gd-pDBI was feasible and could lead to designing new drug delivery systems based on gadolinium (III) with the high loading (compared to the loading of DOX in other MOFs) and low toxicity [76].

A new strategy researched currently is to target cancer cells by magnetic MOFs. MOFs that exhibit magnetic characteristics can be utilized to target the drug to the desired location by applying an external magnetic field source [78]. This method is applicable in the treatment of tumors with a known location [79]. Nimesulide (NIM), an anti-cancer agent used in the treatment of pancreatic [78], colorectal, breast, prostate and other tumors [80], was encapsulated in a three dimensional magnetic MOF [78], to reduce its adverse side effects (mainly gastrointestinal intolerance and ulcers) [81]. The MOF was synthesized using iron oxide (Fe_3O_4) and $Cu_3(BTC)_2$ [78].

First, iron oxide magnetic nanoparticles were synthesized using the procedure reported by Mikhaylova *et al.* [82]. Typical amounts of 2.7 g (10 mmol) of ferrous sulfate ($FeSO_4.7H_2O$) and 2.7 g (10 mmol) of ferric trichloride ($FeCl_3.6H_2O$) were dissolved in 60 mL of distilled water. Drops of ammonia solution ($NH_3.H_2O$, 25%) were added and the entire mixture was stirred at 30°C. Then, the temperature was increased to 80°C for 30 min and Fe_3O_4 nanorods formed and precipitated. The particles were separated by centrifugation, washed 3 times with 30 mL of distilled water and dispersed in ethanol. After the evaporation of ethanol, the concentration of the resulting iron oxide particles was measured at approximately 7 mg/mL [78].

After obtaining Fe_3O_4 nanorods, 0.5 g (2.38 mmol) of BTC was dissolved in 80 mL of an equimolar mixture of ethanol and DMF. Then, 10 mL and 5 mL of ethanol containing Fe_3O_4 particles were added to the BTC mixture, stirred and heated to 70°C to obtain nanocomposites (1) and (2), respectively. Forty mL of copper (II) acetate (0.86 g, 4.31 mmol) aqueous solution was stirred with the mixture at the same temperature for 4 h. The final MOF particles were obtained by centrifugation, washed once with 50 mL of water and three times with 10 mL of ethanol. The two nanocomposites have mainly irregular shapes and their sizes ranging between 50 and 150 nm [78].

Before loading the above nanocomposites, 800 mg of NIM were dissolved in 10 mL of trichloromethane.

Then, 100 mg of the MOF were added to the mixture and stirred in a sealed vessel for 24 h at room temperature. The mixture was filtered, washed twice with 5 ml of trichloromethane and dried at 70°C under vacuum. UV-vis spectroscopy was used to determine the amounts of NIM encapsulated in the pores of the magnetic MOF. These amounts were found to be 0.172 and 0.201 g of NIM per gram of composites (1) and (2), respectively, which are similar to loading results obtained in other MOFs [78].

Release experiments were then conducted at 37 ± 0.2°C for nanocomposite (1). The loaded particles (100 mg) were suspended in 100 mL of physiological saline and the mixture was stirred. Five mL were removed during the experiment and the same volume was replenished by fresh saline. The release profile was divided into three phases [78].

At the beginning, the release was rapid with approximately 20% occurring during the first 4 h (diffusion and dissolution of drug in aqueous medium). Then, the release slowed down and 70% of the drug release took place within 7 days (desorption, diffusion and dissociation of drug from the framework pores to the aqueous solution). Finally, the remaining percentage (10%) was released very slowly taking approximately 4 days [78]. This slow phase of release is attributed to the interaction between the drug molecules and the unsaturated bonds in the framework [83].

The magnetic drug delivery system described above represents an effective method of encapsulating a drug and targeting it directly to the desired location in the body by applying an external magnetic field. Although there were successful efforts to design a magnetic targeted drug delivery based on mesoporous silica (e.g. MCM-41) particles, the complicated and high cost synthesis of these carriers limited their efficiency and feasibility compared to MOFs [78].

Most recently, amorphous Zr-based MOFs (UiO66) have been synthesized and used to encapsulate calcein (a hydrophobic model drug). The toxicity of Zr is low and it is naturally found in the human body (at approximately 300 mg). Amorphous MOFs have disordered network structures; however, they have the original metal-ligand connectivity of the crystalline framework. UiO-66 was synthesized by dissolving 125 mg of $ZrCl_4$ [zirconium(IV) chloride] in 1 mL of HCl and 5 mL of DMF. 123 mg of BDC were dissolved in 10 mL of DMF. The whole solution was placed in a Teflon autoclave and heated at 80°C for 16 h. After that, the resulting mixture was centrifuged at 5,500 rpm for 10 min and the collected particles were washed 3 times with ethanol and DMF. To remove the remaining solvents, the resulting white product was dried at 90°C under vacuum in an oven [84].

The loading was achieved by stirring 20 mg of UiO-66 with 5 mL of a methanol calcein solution at 37°C for 6 days. To separate the loaded drug, the mixture was centrifuged at 5,500 rpm for 20 min and washed twice with methanol. Then, it was centrifuged again for 10 min and dried overnight at 37°C. The amount of calcein loaded was measured by thermogravimetric analysis (TGA) and found to be 4.9 ± 0.2 wt% [mg calcein added / (mg calcein added + mg UiO-66)]. About 0.2 g of the loaded particles were then placed in a stainless steel jar in a Retsch MM200 mill and grinded at 20 Hz using an 8-mm stainless steel ball for 30 min to obtain the amorphous loaded MOFs. The particles sizes of UiO-66 and amorphous UiO-66 were 261 ± 12 and 272 ± 157 nm, respectively, and did not change after calcein loading [84].

Calcein release experiments (from UiO-66 and amorphous UiO-66) were conducted by stirring 3 mg of nanocarriers with 1 mL PBS (pH 7.4) in an incubator at 37°C. The maximum release of calcein from UiO-66 was 97.07 wt% achieved after 48 hours (half of this amount was released after 1.86 h). The model drug release from the amorphous UiO-66 was also studied and showed two different kinetic rates. About 58% of the calcein was released by desorption and diffusion from the MOF within 24 hours (half of this amount was released after 14 h). After 10 days, a significant amount of calcein was found inside the amorphous UiO-66 nanocarriers and the release kinetics shifted to a very slow phase. Maximum release was reached after 30 days and found to be approximately 80% [84].

To investigate the cytotoxicity of empty UiO-66 and amorphous UiO-66, *in vitro* studies were carried out on HeLa cells. IC_{50} was measured after 24 and 48 h and were found to be 1.503 ± 0.154 mg/mL and 1.357 ± 0.088 mg/mL for UiO-66 and amorphous UiO-66, respectively, which are similar to the IC_{50} reported for the Fe-MIL family [84].

The main disadvantage of using amorphous UiO-66 is that it showed the slowest release kinetics reported compared to all other MOFs investigated as drug delivery vehicles. However, the idea of grinding the loaded particles without changing the main metalligand

bonding can be applied for other MOFs to prolong and control the release [84].

Recently, Zheng *et al.* reported the encapsulation of a natural anti-neoplastic agent, namely curcumin (CCM), in ZIF-8 [85]. Several studies have shown that the anti-cancer activity of CCM would inhibit the proliferation and progression of many tumors including breast, pancreatic, colon, head and neck, prostate and other cancers [86]. The main drawback of CCM is the difficulty encountered upon its administration in the systemic circulation, because of its strong hydrophobic nature (poor absorption) and rapid metabolism [85, 87]. To overcome these shortcomings, several nanocarriers including silica nanoparticles [85], liposomes [89], micelles [90] and other particles were used to encapsulate CCM.

Zheng *et al.* developed a new strategy to load the CCM during the synthesis of ZIF-8 nanoparticles. A typical amount of 150 mg of zinc nitrate hexahydrate was dissolved in 5 mL of deionized water, whereas 5 mg of the drug and 330 mg of 2-methyl imidazole were dissolved in 10 mL of methanol. The two mixtures were stirred, and after 1 min the solution became milky indicating the formation of the loaded nanoparticles (CCM@NZIF-8). The loaded nanoparticles were collected by centrifugation at 10,000 rpm for 15 min. Then, they were washed with 20 mL of methanol 3 times and stored as a suspension in 5 mL of methanol for further experiments. After drying the suspended particles, the reaction yield for a single synthesis was found to be 31 mg of CCM@NZIF-8 [85].

To find the CCM content, the dried nanoparticles were decomposed in 0.05 mL of 2 M HCl and the resulting solution was diluted to 2 mL by adding ethanol. The loading efficiency and capability were determined by analyzing the diluted mixture with an UV−visible spectrophotometer and calculated to be 88.2% (mg loaded drug/mg drug fed) and 12.7 wt% (mg loaded drug/mg loaded nanoparticles), respectively. The average diameter of CCM@NZIF-8 was measured to be 119.3 ± 13.6 nm [85].

In vitro experiments were performed to study the release behavior of CCM as follows: 3 mg of CCM@NZIF-8 were added to 2 mL of PBS (pH 5.0 and 7.4) containing 1 wt% Tween-80 in a dialysis bag. Then, the suspension was incubated in 8 mL of PBS solutions. In an acidic medium (pH 5.0), the release reached 43.4% in 2 days, while only 15.6% of the drug was released at neutral pH (in PBS) within the same timeframe. This result confirmed that the acidic environment (such as the pH in tumors) results in the faster release of the drug from ZIF-8 in, which agrees with previous studies [72].

Zheng *et al.* also measured the EC_{50} of the ZIF-8 nanoparticles against HeLa cells for 48 h and found it to be 63.8 μg/mL. This value is higher than that reported previously (45.0 μg/mL) for the same MOF [71]. The same cell line was incubated with CCM@NZIF-8 and CCM for 2 days. The encapsulated drug showed higher cytotoxicity (IC_{50} = 3.0 μg/mL) compared to free CCM (IC_{50} = 5.4 μg/mL) [85].

Furthermore, *in vivo* experiments were conducted on U14 cervical cancer xenograft in Kunming male mice. When the tumor size grew to an approximate size of 200 mm^3, the mice were divided into groups. They were injected 6 times every 2 days for 2 weeks with saline, free CCM (dissolved in a mixture of ethanol and cremophor eL and diluted with sterile saline) and CCM@NZIF-8. The dosage of CCM and CCM@NZIF-8 was 2.5 mg CCM/kg body weight. After two weeks, the tumors were resected and their weights were found to be 5.98 ± 1.39 g, 3.38 ± 0.9 g, and 0.9 ± 0.23 g, after treatment with saline, free CCM and CCM@NZIF-8, respectively. The study concluded that CCM@NZIF-8 had higher anti-cancer activity *in vivo* and *in vitro* compared to free CCM [85].

The successful encapsulation of CCM in NZIF particles with a high loading capacity and efficiency confirmed the potential use of MOFs as an efficient platform for delivering anti-cancer drugs. Also, the release profile and antitumor efficacy for entrapped CCM were improved compared to the free drug [85].

In 2016, Zhang *et al.* developed a new procedure called the "one pot synthesis" to incorporate DOX in ZIF-8 with the aim of achieving a higher loading compared to the previously reported results [75]. First, an aqueous solution of zinc nitrate hexahydrate was prepared by dissolving 0.2 g of the metal salt in 0.8 g of water at pH 8. Four mL of DOX dissolved in deionized water at three concentrations (2, 6 and 10 mg/mL) were stirred with the metal precursor for 1 min. Then, 2 g of 2-methyl imidazole were dissolved in 8 g of deionized water and added gradually to the previous mixture [91].The whole mixture was stirred for 15 min and the loaded particles (DOX@ZIF-8) were collected by centrifugation. They were washed 3 times with a mixture of water and methanol and dried under vacuum at ambient temperature. The loading percentages were calculated using an UV-visible spectrophotometer and

found to be 4.0, 14 and 20 wt% (mg DOX/mg loaded ZIF-8) for the DOX concentrations of 2, 6 and 10 mg/mL, respectively. The sizes of the particles ranged 70-300 nm [91].

The release study was carried out for 20 wt% loaded ZIF-8 as follows: 10 mg of the dried particles were suspended in 20 mL of PBS containing 10 vol% of fetal bovine serum (FBS) at different pH values (4.0, 5.0, 6.0, 6.5 and 7.4) at 37°C under shaking at 150 rpm. At certain time points, 1 mL of the supernatant was taken and its fluorescence was measured using an UV-visible spectrophotometer and returned to the original release medium. There was no significant release detected after 15 days at pH ≥ 6.5, while 95% of the drug was released steadily at pH 5.0 and 6.0 after 7-9 days (the release increased by only 2% during this 2 days interval) [91].

In addition, the effect of the pH environment on the drug release was investigated using a different procedure. Typically, 10 mg of the loaded MOF were added to PBS containing 10 vol% of FBS and kept for a week. Then, HCl drops (0.6 M) were added to adjust the pH to 6.5 and the resultant mixture was left for another week. Finally, the pH of the solution was adjusted to 6.0, 5.0 and 4.0 over 3 days. To determine the release behavior at the different pH values examined in the study, the same steps mentioned above were followed. The release was also insignificant at higher pH values (7.4 and 6.5) and increased remarkably to reach around 20, 70 and 100% at pH values of 6.0, 5.5 and 5.0, respectively [91].

The cytotoxicity values of free and encapsulated DOX were compared using several breast cancer cell lines (MCF-7, MDA-MB-231 and MDA-MB-468). The cell lines were treated with different doses of equivalent concentrations of DOX and DOX@ZIF-8 for 24 h and the results showed higher cytotoxicity of DOX@ZIF-8 compared to free DOX. When 0.1 μg/mL of DOX and 0.5 μg/mL of DOX@ZIF-8 were used, the percentages of the mitochondrial function decreased from its original value (100%) to 16, 20 and 43% in MDA-MB-231, MDA-MB-468 and MCF-7 cells, respectively. However, at lower concentrations, the loaded and free DOX showed only slight effects on the cells. At concentrations of 0.2 μg/mL of DOX and 1.0 μg/mL of DOX@ZIF-8, the percentages of the mitochondrial function decreased to below 10% [91].

Yang *et al.* introduced a new procedure to use nanoMOFs as drug vehicles gated by nanovalves. Their aims were to trigger drug release in a controlled manner and avoid premature release [92]. The MOF (UMCM-1-NH_2) was prepared by dissolving 3.21 g of $Zn(NO_3)_2 \cdot 6H_2O$, 0.490 g of NH_2-BDC and 0.424 g of H_3BTB in 100 mL of DMF [93]. Each 10 mL of the solution were poured in a scintillation vial and heated in an oven at 85°C for 2 days. The collected crystals were washed with DMF, soaked in dichloromethane for 1day, rinsed and soaked again for 3 days. Then, the soaked particles were dried under vacuum for 12 h. Then, 56 mg of the dried MOF particles were suspended in 10 mL of DMF and 0.0349 g of 1-(6bromohexyl)pyridinium bromide (Py) were added to the suspension. The solution was stirred for 55 h at elevated temperatures (70-150 °C). Then, it was centrifuged and the collected particles (UMCM-1-NH-Py) were washed 3 times with DMF and ethanol. After drying the particles, they were washed 3 times with chloroform and then soaked for 3 days [92].

Ten mg of UMCM-1-NH-Py were suspended in a solution of 1 mM rhodamine 6G (Rh6G) dissolved in neutral PBS. Then, 30 mg of carboxylatopillar[5]arene (CP5) were added to the mixture and stirred for 48 h. CP5 macrocycles surrounded the pyridinium stalks and formed movable caps of the nanocarriers. The loadedcapped-MOF particles were washed with water, centrifuged and dried under vacuum. Their particle diameter was measured to be 102.9 ± 4 nm. The encapsulation efficiency without CP5 caps was found to be much lower (5 μm/g) than with capping (61 μm/g) [92].

The release behavior was investigated by suspending 1 mg of the loaded capped UMCM-1-NH-Py in PBS under stirring at different pH values or by adding methyl viologen salts. The caps were broken at lower pH and the nanocarriers started releasing the model drug. They did not show any release at basic and natural pH; which means that the premature release of the model agent was prevented. After 80 min and at pH 5.0 the release reached 22%, whereas it increased significantly at pH 2.0 to reach about 88%. Methyl viologen salts were also added at different concentrations. It was found that the higher the concentration, the faster the release (it reached approximately 65% after 140 min when 8.7 μm viologen were added, while 35% was released at 0.87 μm) [92].

In the meantime, DOX hydrochloride was loaded (instead of the model drug) using the same steps described above. As is the case with the Rh6G, the loaded capped MOF did not release the DOX at neutral

and acidic pH. At pH 2.0, the release increased with time to reach 55% after 450 min. Additionally, *in vitro* experiments were conducted using UMCM-1-NH-Py and CP5-capped UMCM-1-NH-Py to determine the cytotoxicity on normal human kidney (HEK) 293 cells. Both MOFs (capped and uncapped) showed insignificant cytotoxicities even at the high concentration examined (50 μg/mL) [92].

It was concluded that these nanocarriers were pHsensitive and succeeded in inhibiting premature leakage; which implies a reduction in its effects on normal cells [92].

Another example of attaching supramolecular gates on MOF surface was carried out by Yang *et al.* to encapsulate 5-FU [94]. The MOF (UiO-66-NH_2) was synthesized by dissolving 1.50 g of $ZrCl_4$ and 1.56 g of NH2-BDC in 180 mL of DMF at ambient temperature. This mixture was heated in an oven at 80°C for 12 h and then the temperature was increased to 100°C for 24 hours. The resulting particles were collected by filtration and washed with ethanol while heated in a water bath at 60°C for 3 days. The final produced particles were filtered and dried at 75°C under vacuum for 12 h. About 28 mg of dried UiO-66-NH_2, 0.02 g of 4dimethylaminopyridine, 0.08 g of dicyclohexylcarbodiimide and 0.04 g of quaternary ammonium salt (Q) stalks were stirred in 1 mL of DMF at 40°C for 72 h. The resulting particles were collected by centrifugation. Then, they were washed 3 times with warm DMF and water and dried under vacuum to obtain UiO-66NH-Q [94].

The drug loading was performed by suspending 3 mg of UiO-66-NH-Q in 1 mL of 3.3 mM aqueous 5FU at room temperature for 12 h. After that, 34 mg of CP5 were added to the resulting mixture and stirred for 48 h at room temperature. The loaded capped particles were centrifuged, washed with deionized water and dried under vacuum. The size of the loaded particles ranged between 100-200 nm. The encapsulation efficiency of the capped nanocarriers was measured to be 115 μmol/g, while it was only 42 μmol/g for uncapped particles [94].

Release experiments were conducted by suspending 1 mg of the loaded capped UiO-66-NH-Q in deionized water while being stirred. The capped nanocarriers were activated by adding a competitive binding agent of Zn^{2+} or heating. The binding agent was added at different concentrations and the maximum release percentage, achieved after 100 min, was found to be approximately 70% at 10 mM. At low concentration of Zn^{2+} ions (comparable to the concentration of Zn^{2+} ions in the extracellular fluids) the release of 5-FU was only 5%; which confirms the role of the competitive binding agent in activating the release with slight premature leakage [94].

Release kinetics were also studied at 25 and 37°C. It was found that at both temperatures the premature release was not noticeable; however the nanocarrier showed a relatively faster premature release at 37°C during the first 100 min. After 10 h, the percentage of release was measured at approximately 12% only. When the release was triggered by external heating to 60°C, it increased to approximately 70% after 10 h. The cytotoxicity level was determined by treating human kidney 293 cells with different concentrations of UiO-66-NH-Q and capped UiO-66-NH-Q. Both nanocarriers showed insignificant cytotoxicity even at high concentration (50 μg/mL). The proposed drug delivery system succeeded in triggering the release either by adding a competitive binding agent of Zn^{2+} or external heating [94].

The same research group reported a new technique to trigger the 5-FU release either by using Ca^{+2} ions or changing the pH or the temperature. First, UiO-66-NHQ was prepared using the procedure mentioned above. Then, 3 mg of the nanocarrier were suspended in 1mL of 3.3 mM aqueous 5-FU and the mixture was then exposed to ultrasound. About 48 mg of CP5 were added to the mixture and stirred for 12 h. The capped MOF particles were separated by centrifugation, washed twice with deionized water and dried in a vacuum oven for 24 h. The encapsulation efficiency without capping was calculated to be 42 mmol/g which is considerably lower than the capped MOF (247 mmol/g) [95].

To study the release, 1 mg of the loaded capped UiO-66-NH-Q was suspended in aqueous solution under stirring. At pH 5.0, the gates (caps) were opened and they started releasing the encapsulated drug (18% of it was released after 1 h). When the pH was lowered to 4.0, 54% was released during the same period of time. As expected, at neutral pH the release was considerably lower (less than 5%). The release was also observed by adding different amounts of Ca^{2+}. After 160 min, the maximum drug release (80%) was achieved at the highest concentration studied. At a concentration of 1 mM Ca^{2+} ions (comparable to the concentration of Ca^{2+} ions in the extracellular fluids) the release of 5-FU was only 5%. The effect of increasing the temperature was

also investigated. At 25 and 37°C the release percentage was very low (less than 5%) after 10 h, whereas it increased to approximately 23% at 60°C [95].

In vitro experiments were carried out on human embryonic kidney 293 cells and both nanomaterials (capped and uncapped) showed negligible cytotoxicity at high concentration (50 μg/mL). In conclusion, the described drug delivery system represents an viable approach to avoid the premature release. The release can be triggered by adding Ca^{2+} ions at high concentrations, lowering the pH or external heating [95].

The examples detailed above show the promise of using MOFs as drug delivery vehicles in cancer treatment with higher loading capacities and controlled release.

2.5. The Virtues and Challenges of MOF-based Drug Delivery Systems

There are unique features that endorse the use of MOFs as platforms in drug delivery compared with organic (e.g. liposomes and micelles) and inorganic (e.g. traditional zeolites, mesoporous silica and carbon tubes) nanocarriers [34, 84]. Generally, organic nanomaterials can load different agents; but they are not as efficient in releasing the encapsulated drug in a controlled manner. On the other hand, inorganic carriers have the ability to control the release due to their wellordered structures, but with less loading capacities. In contrary, the examples listed above showed that MOFs are capable of tackling the shortcomings of organic and inorganic carriers showing significantly higher drug loading capacities and controlled delivery (a longer sustained release). This can be attributed to the ability of MOFs to be tuned and functionalized by varying the building blocks (metal ion and organic linker) to obtain frameworks with different pore sizes and morphologies [96, 97].

The biocompatibility, toxicity and stability of MOFs still need to be researched before their practical use in the biomedical field [34, 56]. Other challenges that need to be addressed include the prevention of agglomeration of the nanoparticles as well as controlling the release and stability of the particle sizes in different media. Additionally, further *in vivo* experiments are needed to investigate whether and how the MOFs are able to cross the natural barriers and the most efficient route of administration before their use clinically. Other MOF characteristics that need to be researched are the biodistribution, targeting and biodegradability mechanisms once these carriers are injected in a patient. A full understanding of these aspects is very important to achieve a drug delivery system that employs MOFs and can be practically utilized in clinics and hospitals [56, 96].

CONCLUSION

Cancer is one of the deadliest diseases of the 21st century and is caused by the uncontrollable growth of cells which can adversely affect the organ's functions. The traditional treatment of solid cancerous tumors was surgically resecting them. However, the complete resection and excision of the tumor is not guaranteed, giving a chance to some of the diseased cells to regrow, migrate and metastasize. After gaining a better understanding of tumor growth, "chemotherapy" which is defined simply as treating diseases with chemicals was introduced into cancer clinics. The addition of chemotherapy regimens to traditional cancer treatments could solve the above mentioned drawback. However, these chemotherapies have their own disadvantages including poor targeting specificity, burst effects and insufficient information about the drug disposition in the body (poor pharmacokinetics). Over the past two decades, different nanocarriers have been researched to encapsulate and selectively target these anti-neoplastic agents. These nanomaterials are non-toxic, stable in *in vitro* and *in vivo* environments, biodegradable and have controllable drug distribution and release. Among the recent nanoparticles investigated as effective drug carriers are MOFs which have well-known crystalline structures and high porosity. They also possess flexibility to be formed and tuned by combining different metal ions with organic ligands to achieve the desired structures and sizes that can be used in cancer nanotherapy. The first MOFs to be investigated as drug delivery carriers belong to the MIL family, synthesized using carboxylic acid groups and trivalent metals. This paper details the use of MOFs to encapsulate chemotherapeutic agents and model drugs effectively including ethoxysuccinato-cisplatin (ESCP) loaded in a functionalized Fe-MIL-101, TPT loaded in Fe-MIL-100, busulfan loaded in MIL-88A, MIL-89,
MIL-53 and MIL-100, doxorubicin loaded in Fe-MIL100, fluorescein, DOX and camptothecin loaded in ZIF-8, DOX loaded in Gd-pDBI, calcein loaded in UiO-66 and amorphous UiO-66 and others.

The promising results of loading high concentrations of chemotherapeutic drugs in numerous MOFs and

releasing these agents in a controlled manner open new treatment prospects in our fight against cancer. However several challenges need to be addressed before introducing these drug delivery systems in a clinical setting.

CONFLICT OF INTEREST

The author(s) confirm that this article content has no conflict of interest.

ACKNOWLEDGEMENTS

Declared none.

REFERENCES

[1] Sudhakar, A., History of Cancer, Ancient and Modern Treatment Methods. *Journal of Cancer Science & Therapy* **2009,** *1* (2), 1-4.

[2] Jemal, A.; Bray, F.; Center, M. M.; Ferlay, J.; Ward, E.; Forman, D., Global Cancer Statistics. *A Cancer Journal for Clinicians* **2011,** *61* (2), 69-90.

[3] Shewach, D. S.; Kuchta, R. D., Introduction to Cancer Chemotherapeutics. *Chemical Reviews* **2009,** *109* (7), 2859-2861.

[4] Lindsey , T. A.; Bray, F.; Siegel, R. L.; Ferlay, J.; Tieulent, J. L.; Jemal, A., Global Cancer Statistics, 2012. *A Cancer Journal for Clinicians* **2015,** *65*, 87-108.

[5] Sönmez, Ö. U.; Yalçın, Z. G.; Karakeçe, E.; Çiftci, I. H.; Erdem, T., Associations between Demodex species infestation and various types of cancer. *Acta Parasitologica* **2013,** *58* (4), 551-555.

[6] Bradbury, R. H., *Cancer*. Springer-Verlag Berlin Heidelberg: Alderley Park, 2007.

[7] A.B.Pardee, Cancer Cells and Normal Cells. *American Philosophical Society* **1976,** *120* (2), 87-92.

[8] Zink, D.; Fischer, A. H. ; Nickerson, J. A., Nuclear structure in cancer cells. *Nature Review Cancer* **2004,** *4* (9), 677-687.

[9] M.G.P.Stoker, The Leeuwenhoek Lecture, 1971: Tumour Viruses and the Sociology of Fibroblasts *The Royal Society* **1972,** *181* (1062), 1-17.

[10] Josef, N. F.; Trnka , F., Proenzyme Therapy of Cancer*. *Anticancer Research* **2005,** *25*, 1157-1178.

[11] Tobey, R. A.; Ley, K. D., Iso- leucine Mediated Regulation of Genome Replication in Various Mammalian Cell Lines. *Cancer Research* **1971,** *31*, 46-51.

[12] Chorawala, M. R.; Oza, P. M.; Shah, G. B., Mechanisms of Anticancer Drugs Resistance: An Overview. *International Journal of Pharmaceutical Sciences and Drug Research* **2012,** *4* (1), 1-9.

[13] Bae, Y. H.; Mrsny, R. J.; Park, K., *Cancer Targeted Drug Delivery: An Elusive Dream*. Springer Science+Business Media: New York, 2013.

[14] Chu, E.; DeVita, V., A History of Cancer Chemotherapy. *American Association for Cancer* **2008,** *68* (21), 86438653.

[15] Strebhardt, K.; Ullrich, A., Paul Ehrlich's magic bullet concept: 100 years of progress. *Nature Reviews | Cancer* **2008,** *8*, 473-480.

[16] Mier, W.; Hoffend, J.; Haberkorn, U.; Eisenhut, M., Current Strategies in Tumor-Targeting. In *Apoptotic Pathways as Targets for Novel Therapies in Cancer and Other Diseases*, Springer: Heidelberg, 2005; pp 343-355.

[17] Papac, R. J., Origins of Cancer Therapy. *Yale Journal of Biology and Medicine* **2001,** *74*, 391-398.

[18] Dong , Q.; Barsky, D.; Colvin, M. E.; Melius, C. F.; Ludeman , S. M.; Moravek , J. F.; Colvin , O. M.; Bigner, D. D.; Modrich , P.; Friedman, H. S., A structural basis for a phosphoramide mustard-induced DNA interstrand crosslink at 5'-d(GAC). *Proc. Natl. Acad. Sci.* **1995,** *92*, 1217012174.

[19] Jacobson, W., The Mode of Action of Folic Acid Antagonists on Cells. *J. Physiol.* **1954,** *123*, 603-6I7.

[20] Albushra , Y.; Ahmed, A. R.; Hasan, Y., Prevention and Management of High Dose Methotrexate Toxicity. *J. Cancer Sci. Ther.* **2013,** *5* (3), 106-112

[21] Pullarkat, S. T.; Stoehlmacher, J.; Ghaderi, V.; Xiong, Y.P.; Ingles, S. A.; Sherrod, A.; Warren, R.; Tsao-Wei, D.; Groshen, S.; Lenz, H.-J., Thymidylate synthase gene polymorphism determines response and toxicity of 5-FU chemotherapy. *The Pharmacogenomics Journal* **2001,** *1*, 6570.

[22] Tripodo, G.; Mandracchia, D.; Collina, S.; Rui, M.; Rossi, D., New Perspectives in Cancer Therapy: The BiotinAntitumor Molecule Conjugates. *Medicinal chemistry* **2014**, 1-8.

[23] Wang, X.; Li, S.; Shi, Y.; Chuan, X.; Li, J.; Zhong, T.; Zhang, H.; Dai, W.; He, B.; Zhang, Q., The development of site-specific drug delivery nanocarriers based on receptor mediation. *Journal of Controlled Release* **2014,** *193*, 139153.

[24] Markman , J. L.; Rekechenetskiy, A.; Holler, E.; Ljubimova, J. Y., Nanomedicine therapeutic approaches to overcome cancer drug resistance. *Advanced Drug Delivery Reviews* **2013**, *65*, 1866-1879.

[25] Wang, X.; Yang, L.; Chen, Z.; Shin, D. M., Application of Nanotechnology in Cancer Therapy and Imaging. *CA Cancer J Clin* **2008,** *58*, 97-110.

[26] Tang, M.-F.; Lei , L.; Guo, S.-R.; Huang, W.-L., Recent progress in nanotechnology for cancer therapy. *Chinese Journal of Cancer* **2010,** *29* (9), 775-780.

[27] Reschiglian, P.; Gref, R.; Monti, S.; Manet, I.; Agostoni, V.; Reschigl, P.; Gref, R.; Monti, S., Host-Guest Interactions in Fe(III)-Trimesate MOF Nanoparticles Loaded with Doxorubicin. *Physical Chemistry* **2014,** *118*, 8532-8539.

[28] Agnihotri, J.; Saraf, S.; Khale, A., Targeting : New Potential Carriers for Targeted Drug Delivery System. *International Journal of Pharmaceutical Sciences Review and Research* **2011,** *8* (2), 117-123.

[29] Kanapathipillai, M.; Brock, A.; Ingber, D. E., Nanoparticle targeting of anti-cancer drugs that alter intracellular signaling or influence the tumor microenvironment. *Advanced Drug Delivery Reviews* **2014,** *79–80*, 107-118.

[30] Matsumura , Y.; Maeda, H., A New Concept for Macromolecular Therapeutics in Cancer Chemotherapy: Mechanism of Tumoritropic Accumulation of Proteins and the Antitumor Agent Smancs. *Cancer Research* **1986,** *46*, 6387-6392.

[31] Fang, J.; Nakamura, H.; Maeda, H., The EPR effect: Unique features of tumor blood vessels for drug delivery, factors involved, and limitations and augmentation of the effect. *Advanced Drug Delivery Reviews* **2011,** *63*, 136151.

[32] Mishra, A. K., *Nanomedicine for Drug Delivery and Therapeutics*. John Wiley & Sons: Johannesburg, 2013.

[33] Danhier , F.; Feron , O.; Préat, V., To exploit the tumor microenvironment: Passive and active tumor targeting of nanocarriers for anti-cancer drug delivery. *Journal of Controlled Release* **2010,** *148* 135-146.

[34] Keskin, S.; Kızılel, S., Biomedical Applications of Metal Organic Frameworks. *Industrial and Engineering Chemistry Research* **2011,** *50* (4), 1799-1812.

[35] Furukawa, H.; Cordova, K. E.; O'Keeffe, M.; Yaghi, O. M., The Chemistry and Applications of Metal-Organic

Frameworks. *American Association for the Advancement of Science* **2013,** *341*, 974-986.

[36] C.Huxford, R.; Rocca, J. D.; Lin, W., Metal-Organic Frameworks as Potential Drug Carriers. *Current Opinion in Chemical Biology* **2010,** *14* (2), 262-268.

[37] Macgillivray, L. R., *Metal-Organic Frameworks: Design and Application*. John Wiely & Sons,Inc.: New Jersy, 2010.

[38] Dey, C.; Kundu, T.; Biswal, B. P.; Mallick, A.; Banerjee, R., Crystalline metal-organic frameworks (MOFs): synthesis, structure and function. *Acta Crystallographica Section B* **2013,** *70*, 3-10.

[39] Mukherjee , S.; Vannice, M. A., Solvent effects in liquidphase reactions: I. Activity and selectivity during citral hydrogenation on Pt/SiO2 and evaluation of mass transfer effects. *Journal of Catalysis* **2006,** *243* (1), 108-130.

[40] Gani, R.; Jiménez-González, C.; Constable, D. J. C., Method for selection of solvents for promotion of organic reactions. *Computers and Chemical Engineering* **2005,** *29* (7), 1661-1676.

[41] Hoskins, B. F.; Robson, R., Infinite polymeric frameworks consisting of three dimensionally linked rod-like segments. *Journal of The American Chemical Society* **1989,** *111*, 5962-5964 (Accessed December 07, 2015).

[42] Fujita, M.; Kwon, Y. J.; Washizu, S.; Katsuyuki, O., Preparation, Clathration Ability, and Catalysis of a TwoDimensional Square Network Material Composed of Cadmium(11) and 4,4' Bipyridine. *Journal of American Chemical Society* **1994,** *116* (3), 1151-1152 (Accessed December 20, 2015).

[43] Byrappa, K.; Yoshimura, M., *Handbook of hydrothermal technology : a technology for crystal growth and materials processing* Noyes Publications / William Andrew Publishing, LLC: Norwich, New York, 2001.

[44] Kupplera, R. J.; Timmonsb, D. J.; Fan, Q. R., Potential applications of metal-organic frameworks. *Coordination Chemistry Reviews* **2009,** *253* (23–24), 3042-3066.

[45] Subramanian, S.; Zaworotko, M. J., Porous Solids by Design: [Zn(4,4′-bpy)2(SiF6)]n·xDMF, a Single Framework Octahedral Coordination Polymer with Large Square Channels. *Angewandte Chemie International Edition* **1995,** *34* (19), 2127-2129 (Accessed December 22, 2015).

[46] Yaghi, M.; Li, H., Hydrothermal Synthesis of a MetalOrganic Framework Containing Large Rectangular Channels. *Journal of Ameriacn Chemical Society* **1995,** *117*, 10401-10402 (Accessed December 13, 2015).

[47] Ni, Z.; Masel, R. I., Rapid Production of Metal-Organic Frameworks via Microwave-Assisted Solvothermal Synthesis. *American Chemical Society* **2006,** *128* (38), 123941239.

[48] Stock, N.; Biswas, S., Synthesis of Metal-Organic Frameworks (MOFs): Routes to Various MOF Topologies, Morphologies, and Composites. *Chemical Reviews* **2012,** *112* (2), 933-969.

[49] Ameloot, R.; Stappers, L., Patterned growth of metalorganic framework coatings by electrochemical synthesis. *Chemistry of Materials* **2009,** *21* (13), 2580-2582.

[50] Klimakow, M.; Klobes, P.; Thünemann, A. F., Mechanochemical Synthesis of Metal-Organic Frameworks: A Fast and Facile Approach toward Quantitative Yields and High Specific Surface Areas *Chemistry of Materials* **2010,** *22* (18), 5216-5221.

[51] Suslick, K. S.; Price, G. J., Applications of Ultrasound to materials chemistry. *Annu. Rev. Mater. Sci.* **1999,** *29*, 295326.

[52] Horcajada, P.; Serre, C.; Vallet-Regi, M.; Sebban, M.; Taulelle, F.; Féry, G., Metal–Organic Frameworks as Efficient Materials for Drug Delivery. *Angew. Chem. Int. Ed.* **2006,** *45*, 5974-5978 (Accessed November 04, 2015).

[53] Huxford, R. C.; Rocca, J. D.; Lin, W., Metal-Organic Frameworks as Potential Drug Carriers. *Current Opinion in Chemical Biology* **2010,** *14* (2), 262-268.

[54] An, J.; Geib, S. J.; Rosi, N. L., Cation-triggered drug release from a porous zinc-adeninate metal–organic framework. *The American Chemical Society* **2009,** *131*, 83768377.

[55] Schäfer-Korting, M., *Drug Delivery*. Springer-Verlag Berlin Heidelberg: Berlin, 2010.

[56] Horcajada, P.; Chalati, T.; Serre, C.; Gillet, B.; Sebr, C.; Baati, T.; Eubank, J. F.; Heurtaux, D.; Clayette, C.; Kreuz, C.; Chang, J.-S.; Hwang, Y. K.; Marsaud, V.; Bories, P.-N.; Cynober, L.; Gil, S.; Férey, G.; Couvreur, P.; Gref, R., Porous metal–organic-framework nanoscalecarriers as a potential platform for drug delivery and imaging. *Nature Materials* **2010,** *9*, 172-178.

[57] Taylor-Pashow, K. M. L.; Rocca, J. D.; Xie, Z.; Tran, S.; Lin, W., Post-Synthetic Modifications of Iron-Carboxylate Nanoscale Metal-Organic Frameworks for Imaging and Drug Delivery. *American Chemical Society* **2009,** *131*, 14261-14263.

[58] Graf, N.; Lippard, S. J., Redox activation of metal-based prodrugs as a strategy for drug delivery. *Advanced Drug Delivery Reviews* **2012,** *64* (11), 993-1004.

[59] Florea, A.-M.; Büsselberg, D., Cisplatin as an Anti-Tumor Drug: Cellular Mechanisms of Activity, Drug Resistance and Induced Side Effects. *Cancers* **2011,** *3*, 1351-1371.

[60] Wang, G.-S.; Zhang, H.-Y.; Liu, Y., Preparation and characterization of inclusion complexes of topotecan with sulfonatocalixarene. *Journal of Inclusion Phenomena And Macrocyclic Chemistry* **2011,** *69*, 85-89.

[61] Nunzio, M.; Agostoni, V.; Cohen], B.; Gref, R.; Douhal, A., A "Ship in a Bottle" Strategy To Load a Hydrophilic Anticancer Drug in Porous Metal Organic Framework Nanoparticles: Efficient Encapsulation, Matrix Stabilization, and Photodelivery. *J. Med. Chem.* **2014,** *57* (2), 411420.

[62] Huang, X.; Brazel, C. S., On the importance and mechanisms of burst release in matrix-controlled drug delivery systems. *Journal of Controlled Release* **2001,** *73* (2-3), 121-136.

[63] Andersson, B. S.; Lima, M. d.; Thall, P. F.; Wang, X.; Couriel, D.; Korbling, M.; Roberson, S.; Giralt, S. G.; Pierre, B.; Russell, J. A.; Shpall, E. J.; Jo, R. B.; Champlin, R. E., Once Daily i.v. Busulfan and Fludarabine (i.v. Bu-Flu) Compares Favorably with i.v. Busulfan and Cyclophosphamide (i.v. BuCy2) as Pretransplant Conditioning Therapy in AML/MDS. *Biology of Blood and Marrow Transplantation* **2008,** *14*, 672-684.

[64] Mei, Q.; Li, F.; Quan, H.; Liu, Y.; Xu, H., Busulfan inhibits growth of human osteosarcoma through miR-200 family microRNAs *in vitro* and *in vivo*. *Cancer Science* **2014,** *105* (7), 755-762.

[65] Chalat, T.; Horcajada, P.; Couvreur, P.; Serre, C.; Yahia, M. B., Porous metal organic framework nanoparticles to address the challenges related to busulfan encapsulation. *Nanomedicine* **2011,** *6* (10), 1683-1695.

[66] Takemura , G.; Fujiwara, H., Doxorubicin-Induced Cardiomyopathy From the Cardiotoxic Mechanisms to Management. *Progress in Cardiovascular Diseases* **2007,** *49* (5), 330-352.

[67] Liu, Z.; Cheung, R.; Wu, X. Y.; Ballinger, J. R.; Bendayan, R.; Rauth, A. M., A study of doxorubicin loading onto and release from sulfopropyl dextran ion-exchange microspheres. *Controlled Release* **2001,** *77* (3), 213-224.

[68] Chatterjee, K.; Zhang, J.; Honbo, N.; S. Karliner, J., Doxorubicin Cardiomyopathy. *Cardiology* **2010,** *115* (2), 155-162.

[69] Chen, Y.; Wan, Y.; Wang, Y.; Zhang, H.; Jiao, Z., Anticancer efficacy enhancement and attenuation of side effects of doxorubicin with titanium dioxide nanoparticles. *International Journal of Nanomedicine* **2011,** *6*, 2321-2326.

[70] Krishna, R.; Mayer, L. D., Multidrug Resistance (MDR) in Cancer - Mechanisms, Reversal Using Modulators of MDR and the Role of MDR Modulators in Influencing the Pharmacokinetics of Anticancer Drugs. *European Journal of Pharmaceutical Sciences* **2000,** *11* (4), 265-283.

[71] Zhuang, J.; Kuo, C.-H.; Chou, L.-Y.; Liu, D.-Y.; Weerapana, E.; Tsung, C.-K., Optimized metal organicframework nanospheres for drug delivery: evaluation of small-molecule encapsulation. *ACS nano* **2014,** *8* (3), 28122819.

[72] Sun, C.-Y.; Qin, C.; Wang, X.-L.; Yang, G.-S.; Shao, K.Z.; Lan, Y.-Q.; Su, Z.-M.; Huang, P.; Wang , C.-G.; Wang, E.-B., Zeolitic imidazolate framework-8 as efficient pHsensitive drug delivery vehicle. *Dalton Transactions* **2012,** *41* (23), 6906–6909 (Accessed March 14, 2015).

[73] Arias, J. L., Novel strategies to improve the anticancer action of 5-fluorouracil by using drug delivery systems. *Molecules* **2008,** *13*, 2340-2369.

[74] Park, K. S.; Ni, Z.; Cote, A. P.; Choi, J. Y.; Huang, R.; Uribe-Romo, F. J.; Chae, H. K.; , M.; , O. M., Exceptional chemical and thermal stability of zeolitic imidazolate frameworks. *PNAS* **2006,** *103*(27), 10186-10191.

[75] Adhikar, C.; Das, A.; Chakrabort, A., Zeolitic imidazole framework (ZIF) nanospheres for easy encapsulation and controlled release of an anticancer drug doxorubicin under different external stimuli: a way toward smart drug delivery system. *Molecular Pharmaceutics* **2015,** *12* (9), 3158-3166.

[76] Kundu, T.; Mitra, S.; Patra, P.; Goswami, A.; Diaz, D. D.; Banerjee, R., Mechanical Downsizing of a Gadolinium(III)based Metal-Organic Framework for Anticancer Drug Delivery. *Chemistry - A European Journal* **2014,** *20*, 1051410518 (Accessed October 25, 2015).

[77] Long , G.; Meek, M. E.; Lewis, M. *N,N-Dimethylformamide*; World Health Organization: Geneva, 2001.

[78] Ke, F.; Yuan, Y.-P.; Qiu, L.-G.; Shen, Y.-H.; Xie, A.-J.; Zhu, J.-F.; Tian, X.-Y.; Zhang, L.-D., Facile fabrication of magnetic metal–organic framework nanocomposites for potential targeted drug delivery. *J. Mater. Chem.* **2011,** *21* (11), 3843-3848 (Accessed February 23, 2016).

[79] Tran , L. A.; Wilson, L. J., Nanomedicine: making controllable magnetic drug delivery possible for the treatment of breast cancer. *Breast Cancer Research* **2011,** *13* (2), 303.

[80] Rainsford, K. D., *Nimesulide – Actions and Uses*. Birkhäuser Basel: Sheffield, 2005.

[81] Liang, Z.; Liu, J.; Li, L.; Wang, H.; Zhao, C.; Jiang, L.; Qin, G., Effect of nimesulide on the growth of human laryngeal squamous cell carcinoma. *American Journal of Otolaryngology* **2014,** *35* (2), 120-129.

[82] Mikhaylova, M.; Kim, D. K.; Bobrysheva, N.; Osmolowsky, M.; Semenov, V.; Tsakalakos, T.; Muhammed, M., Superparamagnetism of Magnetite Nanoparticles: Dependence on Surface Modification. *Langmuir* **2004,** *20*, 2472-2477.

[83] Gadzikwa, T.; Lu, G.; Stern, C. L.; Wilson, S. R.; Hupp, J. T.; Nguyen, S. T., Covalent surface modification of a metal–organic framework: selective surface engineering via CuI-catalyzed Huisgen cycloaddition. *Chem. Commun.* **2008,** (43), 5493-5495.

[84] Orellana-Tavra, C. A.; Baxter, E. F.; Tian, T.; Bennett, T. D.; Slater, N. K. H.; Cheethamb , A. K.; Fairen-Jimenez, D., Amorphous metal-organic frameworks for drug delivery. *Chemical Communication* **2015,** *51* (73), 13878-13881 (Accessed December 13, 2015).

[85] Zheng, M.; Liu, S.; Guan, X.; Xie, Z., One-Step Synthesis of Nanoscale Zeolitic Imidazolate Frameworks with High Curcumin Loading for Treatment of Cervical Cancer. *ACS Applied Materials and Interfaces* **2015,** *7* (40), 2218122187.

[86] Shanmugam , M. K.; Rane, G.; Kanchi , M. M.; Arfuso, F.; Chinnathambi , A.; Zayed , M. E.; Tan, B. K.; Kumar, A. P.; Sethi, G., The Multifaceted Role of Curcumin in Cancer Prevention and Treatment. *Molecules* **2015,** *20*, 2728-2769.

[87] Anand, P.; Kunnumakkara, A. B.; Newman, R. A.; Aggarwal, B. B., Bioavailability of Curcumin: Problems and Promises. *Molecular Pharmaceutics* **2007,** *4* (6), 807-818.

[88] Chin, S. F.; Iyer, K. S.; Saunders, M.; Pierre, T. G.; Buckley, C.; Paskevicius, M.; Raston, C. L., Encapsulation and Sustained Release of Curcumin using Superparamagnetic Silica Reservoirs. *Chemistry - A European Journal* **2009,** *15*, 5661-5665.

[89] Mourtas , S.; Lazar , A. N.; Markoutsa , E.; Duyckaerts, C., Multifunctional nanoliposomes with curcumine-lipid derivative and brain targeting functionality with potential applications for Alzheimer disease. *European Journal of Medicinal Chemistry* **2014,** *80* 175-183.

[90] Sahu, A.; Kasoju, N.; Bora, U., Fluorescence Study of the Curcumin-Casein Micelle Complexation and Its Application as a Drug Nanocarrier to Cancer Cells. *Biomacromolecules* **2008,** *9*, 2905-2912.

[91] Zheng, H.; Zhang, Y.; Liu, L.; Wan, W.; Guo, P.; Nystrom, A. M.; Zou, X., One-pot Synthesis of Metal−Organic Frameworks with Encapsulated Target Molecules and Their Applications for Controlled Drug Delivery. *J. Am. Chem. Soc.,* **2016,** *138*, 962-968.

[92] Tan, L.L.; Haiwei , L.; Qiu, Y.C.; Chen, D.-X.; Wang, X.; Pan, R.Y.; Wang, Y.; Zhang, S. X.A.; Wang, B.; Yang, Y.W., Stimuli-responsive metal–organic frameworks gated by pillar[5]arene supramolecular switches. *Chemical Science* **2015,** *6*, 1640–1644.

[93] Wang, Z.; Tanabe , K. K.; Cohen, S. M., Accessing Postsynthetic Modification in a Series of Metal-Organic Frameworks and the Influence of Framework Topology on Reactivity. *Inorg. Chem.* **2009,** *48* (1), 296–306.

[94] Tan, L.-L.; Li, H.; Zhou, Y.; Zhang, Y.; Feng, X.; Wang, B.; Yang, Y.-W., Zn +- Triggered Drug Release from Biocompatible Zirconium MOFs Equipped with Supramolecular Gates. *Small* **2015,** *11* (31), 3807–3813.

[95] Tan, L.-L.; Song, N.; Zhang, S. X.-A.; Li, H.; Wang, B.; Yang, Y.-W., Ca2+, pH and thermo triple-responsive mechanized Zr-based MOFs for on-command drug release in bone diseases. *J. Mater. Chem. B* **2016,** *4*, 135-140.

[96] McKinlay, A. C.; Morris, R. E.; Horcajada, P.; Ferey , G.; Gref, R.; Couvreur, P.; Serre, C., BioMOFs: Metal-Organic Frameworks for Biological and Medical Applications. *Angew. Chem. Int. Ed.* **2010,** *49*, 6260-6266.

[97] Cai , W.; Chu, C.-C.; Liu, G.; Wáng, Y.-X. J., Metal–Organic Framework---Based Nanomedicine Platforms for Drug Delivery and Molecular Imaging. *Small* **2015,** *11*(37), 4806-4822.

PMID: 27686655